NASA Contractor Report 174946

Time Dependency of Strainrange Partitioning Life Relationships

Sreeramesh Kalluri and S.S. Manson
Case Western Reserve University
Cleveland, Ohio

August 1984

Prepared for the
Lewis Research Center
Under Contract NAG 3-337

NASA
National Aeronautics and Space Administration

TIME-DEPENDENCY OF SRP LIFE RELATIONSHIPS

INTRODUCTION

Strainrange Partitioning (SRP) is a method developed by Manson, Halford and Hirschberg [1] to determine the cyclic lives of engineering materials used in components subjected to high temperature low cycle fatigue (HTLCF). Conventional SRP recognizes inelastic strainrange as the primary variable governing cyclic life and distinguishes between four different types of strainranges (PP, PC, CC and CP). These generic strainranges constitute the basic waveforms in which creep can be combined with plasticity. However, within each waveform of loading involving creep strain, secondary variables such as creep rate and exposure-time can influence cyclic life in HTLCF. These two secondary variables are not independent of each other. Creep rate is inversely related to the exposure time for failure. Although account is taken in a secondary manner by using modifications based on tensile test ductility and creep test ductility the characterizing SRP relationships are obtained experimentally without regard for the time involved in any one test.

Long-time duration creep-fatigue tests are not only expensive to conduct in the laboratory but it is also difficult to maintain all the controlling parameters (such as temperature, load or strain, etc.) without fluctuations during the entire life time of such a test. Hence most of the tests conducted in the laboratory tend to be short time duration tests with the failure time of the order of a few hours to a few hundred hours. However, in practice jet engine hot section components, and nuclear reactor components which operate at high temperatures, must be designed for several thousand hours and even hundreds of

thousands of hours. Therefore, when creep-fatigue data that are generated at short times in the laboratory are extrapolated to the long time practical applications, the time dependency of life relationships should be properly taken into consideration.

At high temperatures environmental effects, such as oxidation, corrosion, and metallurgical instabilities such as precipitation of new phases and dissolution of the existing phases influence the cyclic life of an engineering component. All of the above phenomena are dependent upon time, and are capable of modifying the mechanical properties (e.g. embrittlement of nickel alloys due to precipitation of sigma phase with time) and the creep response of a material as the time progresses. Since all of these time dependent factors influence the cyclic life of a component, it is very important to consider the time dependency (or the effect of creep rate) of the Strainrange Partitioning life relationships. The goal of this study was to establish quantitatively the effect of exposure time within the CP type of strainrange.

A series of isothermal CP tests with varying exposure times were conducted on 316 SS at 1300°F and 1500°F. Post failure fractography and metallography studies were conducted to establish the effect of the failure time (or creep rate). The experimental technique used, the results of the experiments and the metallurgical studies together with the recently proposed Steady State Creep Rate Modified CP life relationship and the Failure Time Modified CP life relationship are presented in this report.

ALTERNATE METHODS OF TREATING TIME EFFECTS IN HIGH TEMPERATURE LOW CYCLE FATIGUE

a) Frequency Modified Life Equation

The Frequency Modified Life relationship was proposed by Coffin [6] to account for time effects associated with frequency variation during constant strain rate tests at high temperatures. For this equation which is given below, cyclic life, N_f was modified by using frequency, ν associated with that life.

$$\Delta\epsilon = C_2 \left[N_f \nu^{k-1} \right]^{-\beta} + \frac{A'}{E} N_f^{-\beta'} \nu^{k_1'} \qquad (1)$$

$\Delta\epsilon$ = Total strainrange

N_f = Failure life

ν = frequency

$C_2, k, \beta, A', \beta'$ and k_1' are all temperature dependent constants which are evaluated by conducting strain rate controlled tests at various frequencies. In the above equation the effect of wave form of loading on cyclic life was not considered. Further modification of the Frequency Modified Life equation such as Frequency Separation etc., were later proposed in Ref. [6] to include this effect.

b. Ductility Normalized SRP Life Relationships

The Ductility Normalized SRP life relationships are a set of universalized SRP life relationships first proposed by Manson [7], and later modified by Halford, Saltsman and Hirschberg [2]. These life relationships are based on the creep and plastic ductilities which the material exhibits in the environment of interest. The ductility corresponding to the tensile half of the generic loop is used in the

DN-SRP life relationships. Plastic ductility D_p is used for predicting the lives of PP and PC cycles, whereas creep ductility, D_c is used for predicting the lives of CP and CC cycles. Ductility-Normalized SRP life relationships as proposed by Halford, Saltsman and Hirschberg are,

$$N_{pp} = \left[\frac{2\Delta\epsilon_{pp}}{D_p}\right]^{-1.67} \tag{2}$$

$$N_{pc} = \left[\frac{4\Delta\epsilon_{pc}}{D_p}\right]^{-1.67} \tag{3}$$

$$N_{cc} = D_c \left[4\Delta\epsilon_{cc}\right]^{-1.67} \tag{4}$$

$$N_{cp} = D_c \left[5\Delta\epsilon_{cp}\right]^{-1.67} \quad (\textit{transgranular}) \tag{5a}$$

$$N_{cp} = D_c \left[10\Delta\epsilon_{cp}\right]^{-1.67} \quad (\textit{intergranular}) \tag{5b}$$

The Ductility Normalized SRP life relationships can be used in two ways:

(i) Using DN-SRP life relationships only:

In this case, the effect of exposure time is taken into account by using the ductility D_c , or D_p, corresponding to the failure time of the test. These ductility values are used to evaluate the cyclic lives using Eqs. (2)-(5). The variation of ductility with rupture time is obtained from static creep rupture tests in the environment of interest.

(ii) Using DN-SRP life relationships in conjunction with experimentally obtained short-time SRP life relationships:

SRP life relationships can easily be generated in the laboratory for short time duration tests. These life relationships can be extrapolated to long time durations using the Ductility-Normalized life relationships. At a given inelastic strainrange, the following equation can be obtained from Eqs. (2)-(5):

$$\frac{N_{short}}{N_{long}} = \left\{\frac{D_{long}}{D_{short}}\right\}^{a} \qquad (6)$$

where the exponent a is obtained from the appropriate life relation in the short time duration tests.

c) Critique

The Frequency Modified Life equation utilizes continuous cycling data, generated at various frequencies as the baseline data to evaluate the constants of Eq. (1). In doing so, the nature of the strainrange (or waveform of loading) is also varied simultaneously (from PP to a combination involving both PP and CC). The effects of waveform of loading and frequency of loading on cyclic life are combined in Eq. (1). Thus the Frequency Modified Life relationship consists of a combination of two different types of strains (PP and CC), together with the time effects of CC. As a result, it should not be applied to determine the cyclic life when frequency is varied within strainranges such as CP and PC.

The life predictions by DN-SRP life relationships are generally within a factor of 3 of the observed lives. However, DN-SRP life relationships sometimes tend to predict values that are not completely in agreement with the trend observed in the experimental data, as later illustrated in this report.

In view of the above limitations of the previous methods, there is a necessity for another technique, which can quantitatively predict the effect of frequency within different types of waveforms in a distinct manner without mixing the effects of frequency and different types of strainranges on the cyclic life.

THE EFFECT OF FREQUENCY ON CYCLIC LIFE WITHIN A GIVEN WAVEFORM OF LOADING

The Strainrange Partitioning method developed to date accounts for the variation of cyclic life due to different types of waveforms. This is accomplished by considering the following four types of strainranges and the associated life relationships:

$$N_{pp} = A \left[\Delta\epsilon_{pp}\right]^{\alpha} \tag{7a}$$

$$N_{cp} = B \left[\Delta\epsilon_{cp}\right]^{\beta} \tag{7b}$$

$$N_{pc} = C \left[\Delta\epsilon_{pc}\right]^{\gamma} \tag{7c}$$

$$N_{cc} = D \left[\Delta\epsilon_{cc}\right]^{\delta} \tag{7d}$$

where

$\Delta\epsilon_{i,j}$ = generic strainrange

$N_{i,j}$ = cyclic life associated with the generic strainrange

i = p (plasticity), c (creep)

j = p,c

The damage associated with any hysteresis loop containing more than one generic strain range is calculated using the Interaction Damage rule (7) given

below:

$$\frac{F_{pp}}{N_{pp}} + \frac{F_{cc}}{N_{cc}} + \left[\frac{F_{pc}}{N_{pc}} \text{ or } \frac{F_{cp}}{N_{cp}}\right] = \frac{1}{N_f} \tag{8}$$

where

$$F_{i,j} = \frac{\Delta\epsilon_{i,j}}{\Delta\epsilon_{in}} \qquad \begin{matrix} i = p,c \\ j = p,c \end{matrix}$$

$N_{i,j}$ = cyclic life associated with $\Delta\epsilon_{i,j}$, considering $\Delta\epsilon_{i,j} = \Delta\epsilon_{in}$ (Eqs. 7).

N_f = Predicted cyclic life of the hysteresis loop.

The effect of frequency within a given waveform of loading can be accomplished by modifying Eqs. (7). Hence the effect of waveform of loading and the effect of frequency within each waveform are obtained in a distinct manner without changing the nature of strainrange and frequency at the same time.

In the following sections of this report, the effect of frequency within the CP type of strainrange is presented.

(a) Tensile Strain Hold and Stress Hold Tests

CP type of loading is encountered in engineering practice at high temperatures whenever tensile creep is reversed by compressive plasticity. Typical examples of CP type of loading are strain-hold and stress-hold tests in tension. Figure 1 shows a strain-hold hysteresis loop *abcdea*. The vertical line *cd* indicates tensile strain hold at maximum tensile strain. The amount of elastic strain converted into creep strain is indicated by *c'e* during the tensile strain hold. The same amount of creep strain can also be introduced by holding the stress at its maximum value, i.e. a stress-hold at the maximum tensile stress along horizontal line *cd'*; however, the time required to complete loop *abcd'ea* (stress hold at maximum tensile stress) is much smaller than the time required to

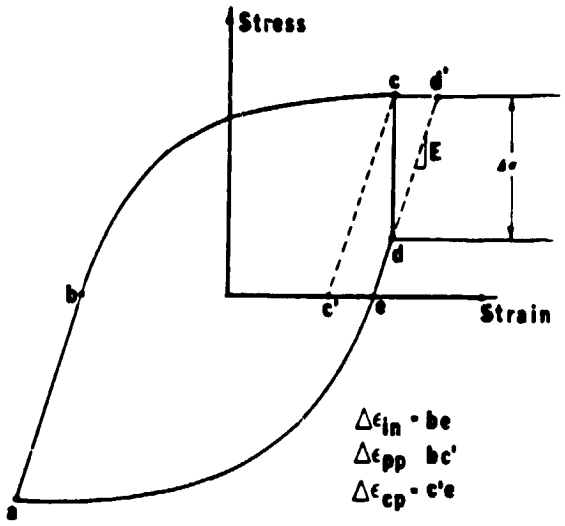

Fig. 1. Comparision of a Tensile Strain Hold Test with a Tensile Stress Hold Test.

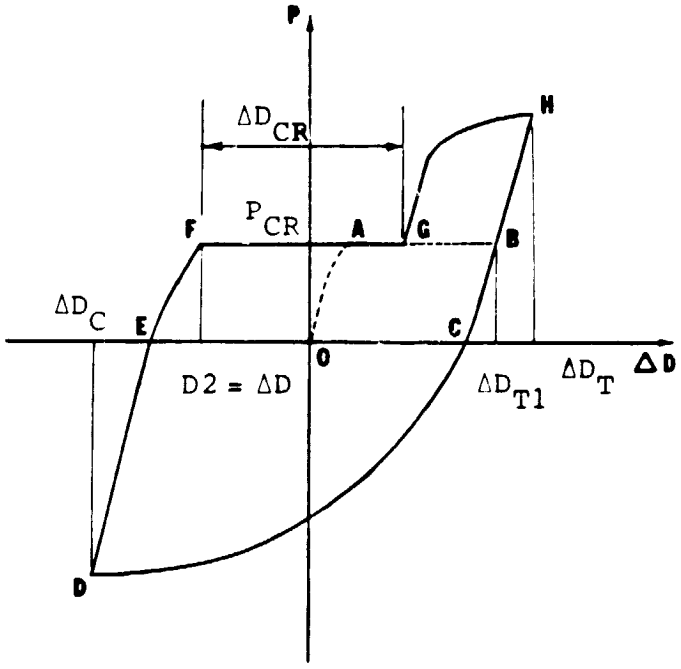

Fig. 2. Schematic Hysteresis Loop of CP Test with a Constant Creep Strain.

complete loop *abcdea* (strain hold) at maximum tensile strain. This is due to the fact that in loop *abcd'ea* (stress hold), the entire amount of creep strain is introduced at the maximum tensile stress, whereas in loop *abcdea* (strain-hold), creep is introduced at progressively decreasing stress levels, the maximum being the same as that of loop *abcd'ea*. The cyclic lives of the above loops can differ substantially due to several reasons such as environmental effects, metallurgical instabilities, etc. Hence it is necessary to develop CP life relationships to account for different exposure times (or creep rates).

CP TESTS WITH VARYING EXPOSURE TIMES

The effect of creep rate (or exposure time) on CP cyclic life was established by conducting a series of uniaxial isothermal tensile stress hold tests. A schematic hysteresis loop of a CP test with constant creep strain is illustrated in Figure 2. The stabilized hysteresis loop is given by *BCDEFGH*. In tension, first a required amount of creep strain (ΔD_{CR}) was imposed at a desired stress level (P_{CR}) and the remaining inelastic strain in tension was imposed by rapidly increasing the load from *G* to *H* to induce plasticity. The load was reversed at *H*, and the specimen was rapidly loaded in compression to *D*, to induce plasticity. The load was reversed again at *D*, and the specimen was loaded in tension up to the creeping stress level. This loop was repeated until failure. Varying exposure times were achieved by introducing creep at different stress levels. Experimental details are presented in a more elaborate manner in Ref. [3].

In all of the tests conducted the ratio of total creep strain to total inelastic strain was maintained at 0.6. At a given inelastic strainrange the total creep strain was maintained at a constant value. (Hence these tests are also referred to as constant creep strain CP tests.) A general purpose computer program

CONCP.BAS was developed in BASIC to conduct these tests. The flowchart, listing of the CONCP.BAS program and sample data input sheet for CONCP.BAS program are presented in Appendix A. Axial stress and the axial inelastic strainrange were obtained from the applied load and diametral displacement using the equations given in Ref. [5].

The total inelastic strainrange of the constant creep strain CP test hysteresis loop was partitioned into generic strainranges CP and PP, considering only the steady state creep strain occurring during the tensile-stress hold as creep strain. The generic CP life was obtained using the Interaction Damage Rule, Eq. (8).

EXPERIMENTAL RESULTS

a) PP life tests:

PP tests were conducted on 316 stainless steel at 1300°F and 1500°F to establish the PP life relationships at these temperatures. These data are shown in Tables I and II for temperatures 1300°F and 1500°F, respectively. The corresponding life relationships are plotted in Figures 3(a) and 3(b).

b) CP tests with varying exposure times:

Uniaxial CP tests with constant creep strain (CONCP.BAS) were conducted at 1300°F (using tubular specimens) and at 1500°F (using solid specimens) on 316 stainless steel. These data are shown in Tables III and IV for 1300°F and 1500°F, respectively. It is clear from the data with the exception of one datum at 1300°F that at a given temperature the cyclic life decreases as the exposure time increases (or as the creep rate decreases).

TABLE I
PP LIFE RELATIONSHIP RESULTS FOR 316 SS AT 1300°F
(F_{pp} = 1)

Specimen #	$\Delta\epsilon_{in}$	N_f
PP		
BYY-148	0.03600	24
BYY-4	0.02140	50
BYY-173	0.01900	207
BYY-232	0.00630	1408
BYY-21	0.00436	553
BYY-22	0.00136	10170

TABLE II
PP LIFE RELATIONSHIP EXPERIMENTS FOR 316 SS AT 1500°F
(F_{pp} = 1)

Specimen #	$\Delta\epsilon_{in}$	N_f
BY-86	0.03058	138
BY-41	0.02010	250
BY-77	0.01996	309
BY-64	0.01189	628

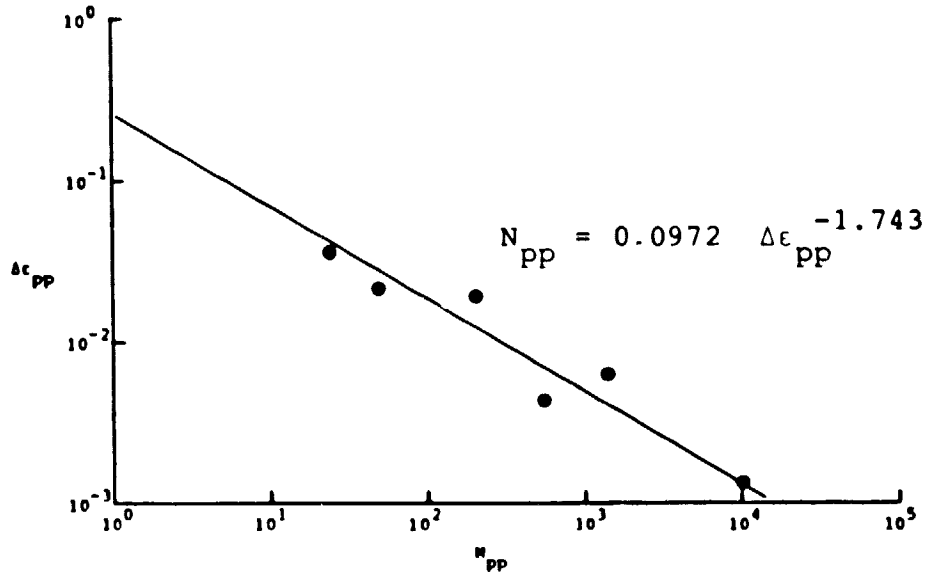

(a) 316 SS at 1300°F.

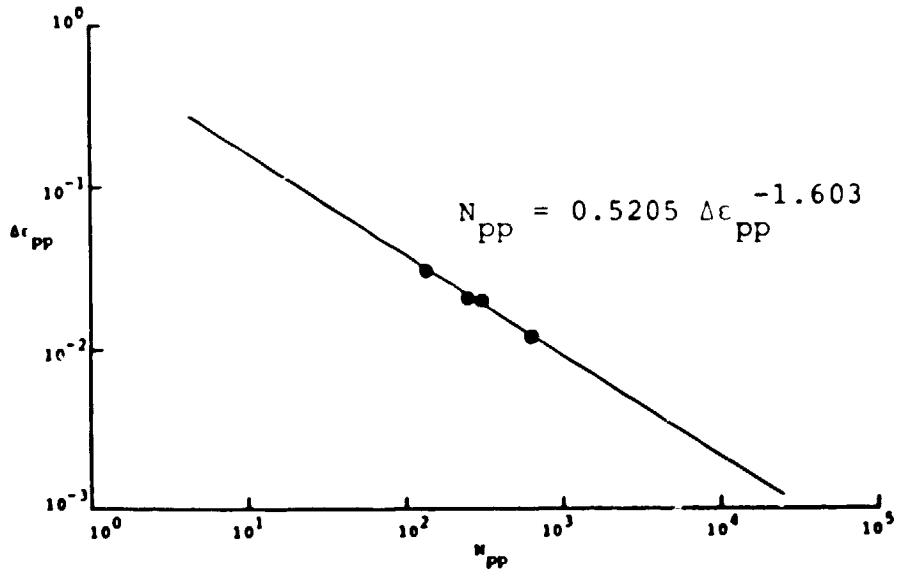

(b) 316 SS at 1500°F.

Fig. 3. PP life Relationships.

TABLE III

RESULTS OF CP TESTS WITH VARYING
EXPOSURE TIMES AT 1300 °F

$\Delta\epsilon_{in} = 0.02$
$F_{pp} = 1-F_{cp}$

Specimen #	F_{cp}	σ_c (KSI)	t_f (hr)	$\dot{\epsilon}_{ss}$ (in/in/min)	N_f	N_{cp}
BYY-218	0.433	36.0	10.1	0.0006062	69	53
BYY-235	0.418	34.0	12.0	0.0004224	52	33
BYY-187	0.417	32.0	27.3	0.0001638	56	37
BYY-239	0.400	30.0	142.3	0.0000431	45	26

TABLE IV

RESULTS OF CP TESTS WITH VARYING
EXPOSURE TIMES AT 1500 °F

$F_{pp} = 1-F_{cp}$

Specimen #	$\Delta\epsilon_{in}$	F_{cp}	σ_c (KSI)	t_f (hr)	$\dot{\epsilon}_{ss}$ (in/in/min)	N_f	N_{cp}
BY-66	0.01	0.419	19.0	7.95	0.001796	215	105
BY-89	0.01	0.222	10.5	169.80	0.000026	124	31
BY-87	0.02	0.543	21.0	3.50	0.004024	94	60
BY-32	0.02	0.458	19.0	4.93	0.002067	80	43
BY-75	0.02	0.364	15.0	21.44	0.000259	58	24
BY-34	0.02	0.315	11.0	95.60	0.000034	46	16
BY-96	0.03	0.565	21.0	2.22	0.003065	29	18
BY-76	0.03	0.335	11.0	101.10	0.000034	22	8

c) Monotonic isothermal creep tests:

A series of isothermal monotonic creep tests were conducted on solid specimens of 316 stainless steel at 1500°F. The results of these experiments were utilized in predicting the cyclic lives of CP tests with constant creep strain using the Ductility-Normalized life relationships [2]. The results of these experiments are tabulated in Table V. The variation of creep ductility, D_c, with the time at 1500°F for 316 stainless steel is shown in Figure 4. The variation of ductility with rupture time is given by:

$$D_c = 2.395 \left[t_r\right]^{-0.14} \tag{9}$$

ANALYSIS OF CP DATA WITH VARYING EXPOSURE TIMES

(1) The raw data of CP tests with constant creep strain, conducted at 1500°F were analyzed using three different types of equations. All the eight data points were used in generating the life relationships.

a) Conventional Manson-Coffin type of equation:

$$N_{cp} = P \left[\Delta\epsilon_{cp}\right]^{Q} \tag{10}$$

where

$\Delta\epsilon_{cp}$ = generic CP strainrange

N_{cp} = generic CP cyclic life

P and Q are material constants

This equation relates the primary variable, i.e. the generic CP strainrange, to the generic CP cyclic life. It does not, however, account for time effects

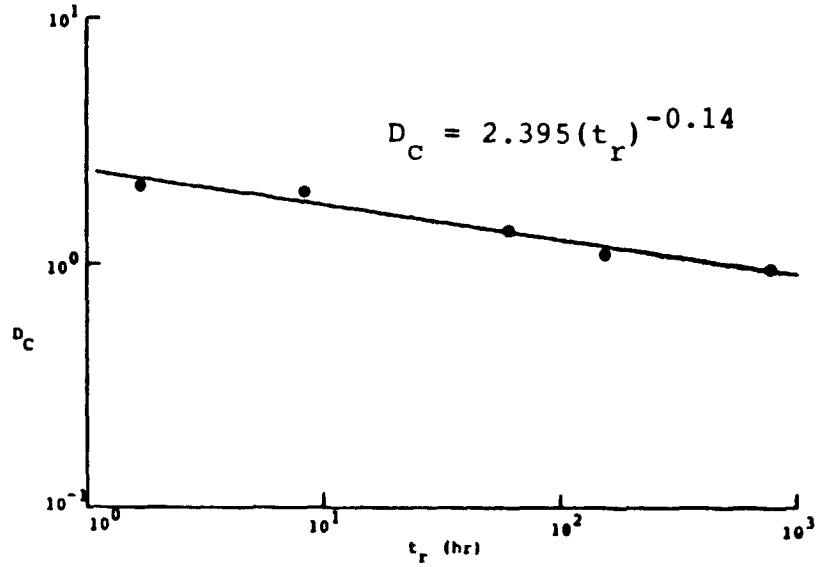

Fig. 4. Creep-Ductility vs. Rupture Time for 316 SS at 1500° F.

TABLE V

RESULTS OF CREEP-RUPTURE EXPERIMENTS
ON 316 STAINLESS STEEL AT 1500°F

Specimen #	σ_c (KSI)	t_f (Hr)	RA%	$D_c = Ln\left[\frac{1}{1-RA}\right]$
BY-78	19.0	1.7	87.5	2.075
BY-61	15.0	8.4	86.3	1.987
BY-95	11.0	61.0	74.9	1.382
BY-74	9.0	154.7	66.4	1.090
BY-62	7.0	784.2	61.8	0.963

TABLE VI

LIFE PREDICTIONS OF CP TESTS WITH VARYING
EXPOSURE TIMES BY CONVENTIONAL SRP

Specimen #	$N_{cp\ pred}$	$N_{cp\ obs}$	$N_{f\ pred}$	$N_{f\ obs}$
BY-66	65	105	140	215
BY-89	65	31	230	124
BY-87	26	60	44	94
BY-32	26	43	51	80
BY-75	26	24	61	58
BY-34	26	16	68	46
BY-96	15	18	24	29
BY-76	15	8	37	22

that can arise within the CP waveform of loading. An equation of the Manson-Coffin type (Eq. (10)) was fitted to the eight data points using linear regression analysis. The resulting CP life relationship is as follows:

$$N_{cp} = 0.1442 \left[\Delta\epsilon_{cp}\right]^{-1.329} \qquad (10a)$$

This equation is plotted in Figure 5(a). It is obvious from the scatter that the above equation simply averages the diverse behavior of the data. Equation (10a) was used to predict the N_{cp} and N_f values corresponding to the strain ranges of the actual data points. These results are shown in Figures 5(b) and 5(c), respectively. The conventional Manson-Coffin equation does not take into consideration the effect of secondary variables such as steady state creep rate (or failure time) within the CP waveform of loading. Hence Eq. (10a) predicts the same cyclic life at a given CP strainrange although the creep rates (hence, failure times) are entirely different. Also, the trend of the back-calculated N_f lives is completely opposite to the experimentally observed trend. The predicted N_f lives were increasing with an increase in the exposure time. This can again be attributed to the lack of consideration of the exposure times. However, the predictions of conventional Strainrange Partitioning CP life equation were in most cases within a factor of 2. These results are presented in Table VI.

b) Steady State Creep Rate Modified CP Life Relationship

Steady state creep rate depends on the temperature and applied stress. Since creep rate was shown earlier to influence the failure time, it is appropriate to incorporate it into the CP life relationship. The resulting life relationship is called the Steady State Creep Rate (SSCR) Modified CP Life Relationship.

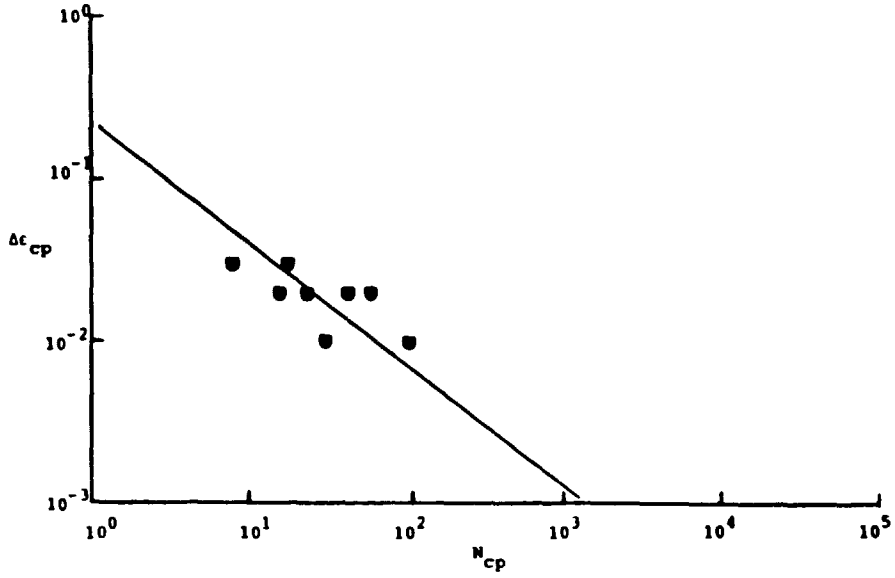

(a). Manson-Coffin equation type of CP Life Relationship at 1500° F for 316 SS.

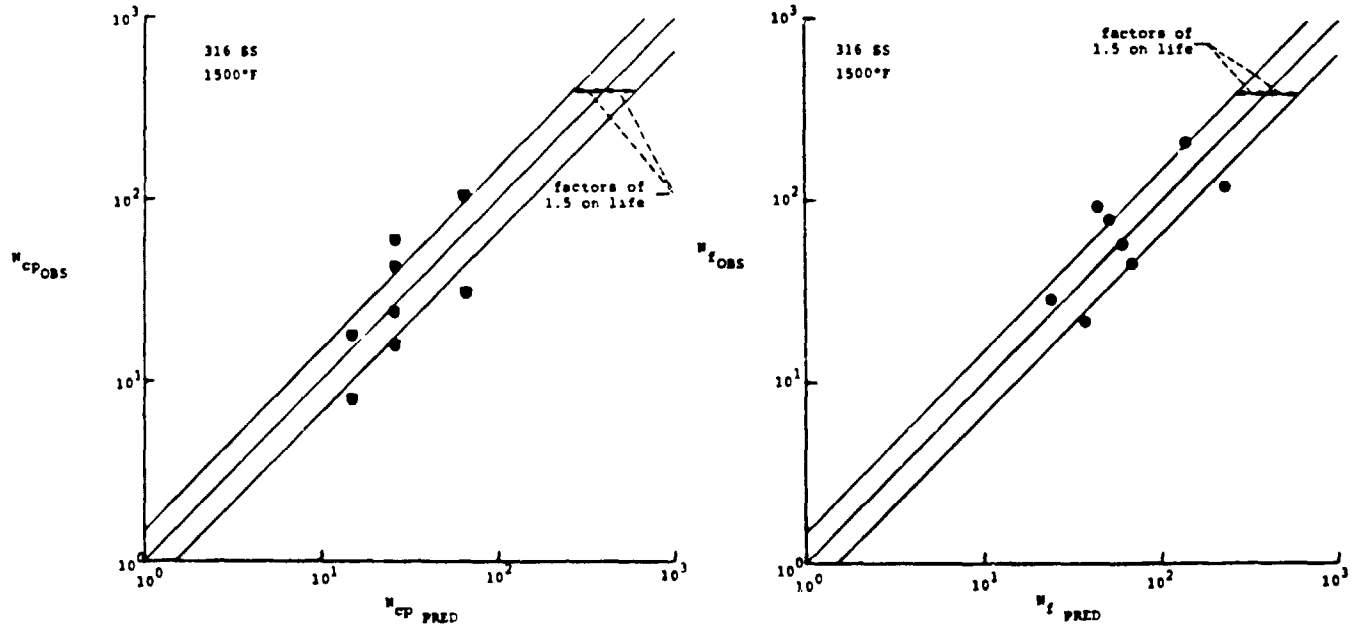

(b). N_{cp} (c). N_f

Fig. 5. Comparision of Observed and Predicted Cyclic lives for CP tests with varying exposure times. Life Predictions based on Manson-Coffin equation type of CP Life Relationship.

$$N_{cp} = A \left[\Delta\epsilon_{cp}\right]^{\alpha} \left[\dot{\epsilon}_{ss}\right]^{\beta} \qquad (11a)$$

A, α, β are material constants; $\dot{\epsilon}_{ss}$ is the steady state creep rate at a given temperature and creep stress. The constants A, α and β were determined for the data presented in Table IV using multiple regression analysis. The details of multiple regression analysis are presented in appendix B of this report. The resulting equation is as follows:

$$N_{cp} = 0.6461 \left[\Delta\epsilon_{cp}\right]^{-1.460} \left[\dot{\epsilon}_{ss}\right]^{0.2557} \qquad (11b)$$

Defining Steady State Creep Rate Modified CP generic life N'_{cp} as,

$$N'_{cp} = \frac{N_{cp}}{\left[\dot{\epsilon}_{ss}\right]^{0.2557}} \qquad (11c)$$

we get $N'_{cp} = 0.6461 \left[\Delta\epsilon_{cp}\right]^{-1.460}$. Equation (11c) is plotted in Figure 6(a). The N_{cp} and N_f values corresponding to $\Delta\epsilon_{cp}$ and $\dot{\epsilon}_{ss}$ of the actual data points were predicted from Eq. (11b). Comparison of observed vs. predicted cyclic life is tabulated in Table VII. These results are also presented in Figures 6(b) and 6(c).

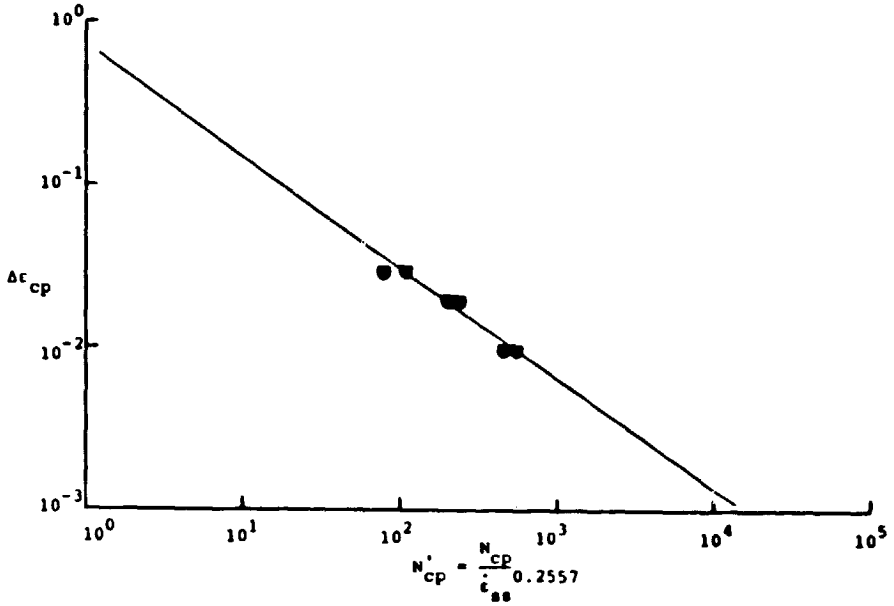

(a). Steady State Creep Rate modified CP Life Relationship at 1500° F for 316 SS.

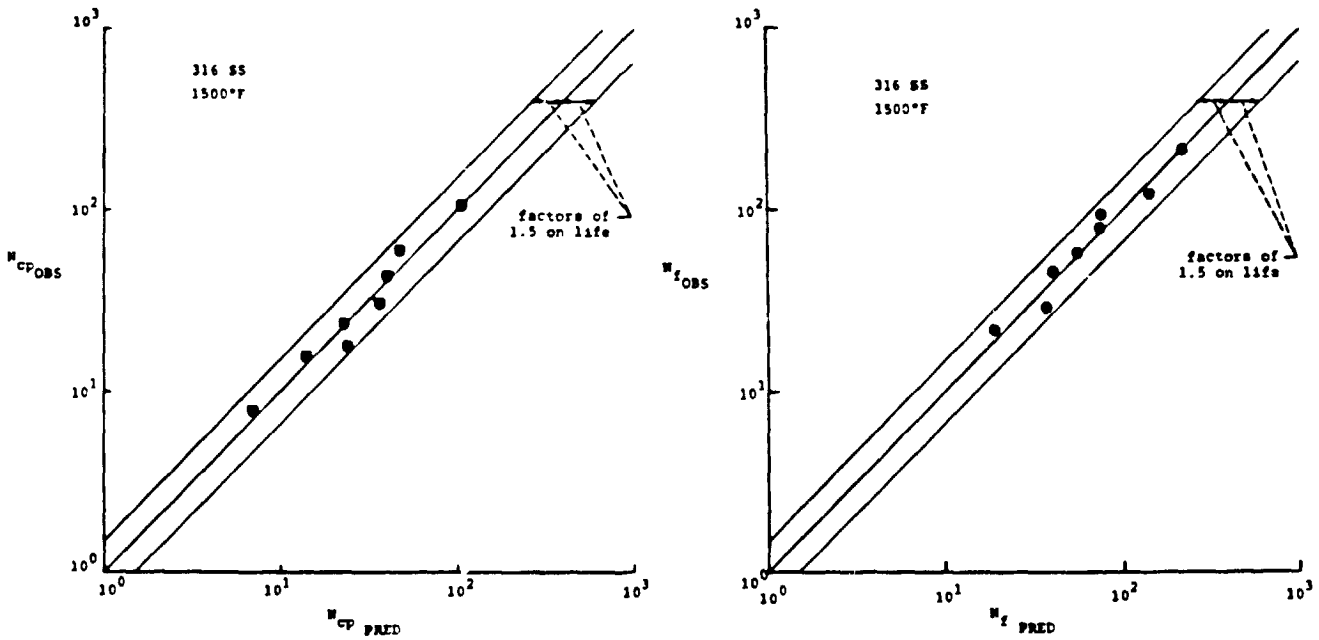

(b). N_{cp} (c). N_f

Fig. 6. Comparision of Observed and Predicted Cyclic lives for CP tests with varying exposure times. Life Predictions based on Steady State Creep Rate modified CP Life Relationship.

TABLE VII

LIFE PREDICTIONS OF CP TESTS WITH VARYING EXPOSURE TIMES
BY STEADY-STATE CREEP RATE MODIFIED CP LIFE EQUATION

Specimen #	$N_{cp\ pred}$	$N_{cp\ obs}$	$N_{f\ pred}$	$N_{f\ obs}$
BY-66	106	105	215	215
BY-80	36	31	140	124
BY-87	47	60	75	94
BY-32	40	43	74	80
BY-75	23	24	55	58
BY-34	14	16	40	46
BY-96	24	18	37	29
BY-76	7	8	19	22

TABLE VIII

LIFE PREDICTIONS OF CP TESTS WITH VARYING EXPOSURE TIMES
BY FAILURE TIME MODIFIED CP LIFE EQUATION

Specimen #	$N_{cp\ pred}$	$N_{cp\ obs}$	$N_{f\ pred}$	$N_{f\ obs}$
BY-66	103	105	210	215
BY-89	37	31	144	124
BY-87	44	60	71	94
BY-32	39	43	72	80
BY-75	24	24	57	58
BY-34	14	16	40	46
BY-96	26	18	40	29
BY-76	7	8	19	22

c) Failure Time Modified CP Life Relationship

This is very similar to the SSCR Modified CP life relationship except that in this case steady state creep rate is replaced by time to failure of the specimen.

$$N_{cp} = B \left[\Delta\epsilon_{cp}\right]^{\gamma} \left[t_f\right]^{\delta} \qquad (12a)$$

where

B, γ, δ are material constants

t_f is the time to failure of the specimen

Again, as in the case of SSCR Modified CP relationship, constants B, γ and δ were determined by multiple regression analysis for the data presented in Table IV. The resulting Failure Time (FT) Modified CP life equation is as follows:

$$N_{cp} = 0.1127 \left[\Delta\epsilon_{cp}\right]^{-1.631} \left[t_f\right]^{-0.3317} \qquad (12b)$$

Failure Time modified CP cyclic life is given by,

$$N''_{cp} = \frac{N_{cp}}{\left[t_f\right]^{-0.3317}} = 0.1127 \left[\Delta\epsilon_{cp}\right]^{-1.631} \qquad (12c)$$

This equation is plotted in Figure 7(a) together with the data points. The observed and predicted cyclic lives are tabulated in Table VIII. These results are also shown in Figures 7(b) and 7(c).

The SSCR Modified CP life relation and the FT Modified CP life relation are not only able to predict the cyclic lives within a factor of 1.5 as compared to conventional SRP life relationship which predicted the lives within a factor of 2, but their predictions show a trend that is consistent with the experimentally observed behavior. This establishes the fact that there is a time effect within the

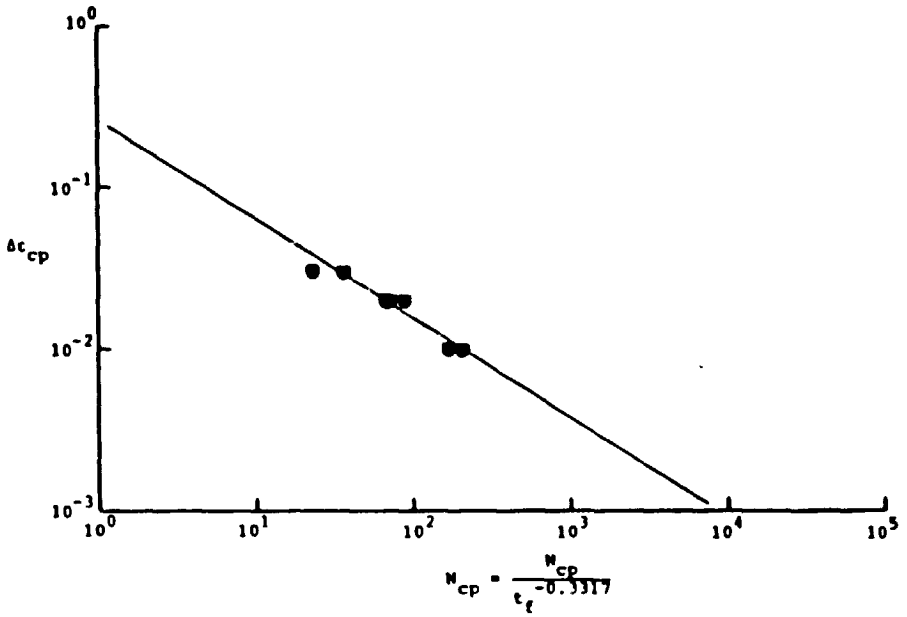

(a). Failure Time modified CP Life Relationship at 1500° F for 316 SS.

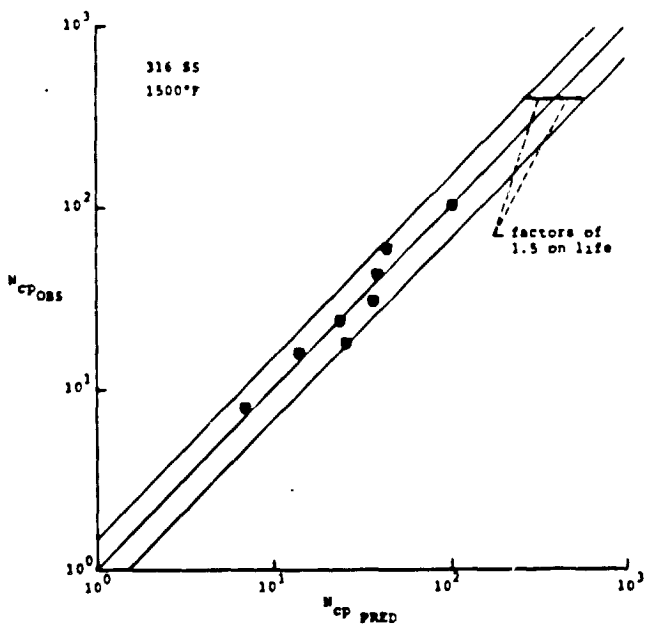

(b). N_{cp}

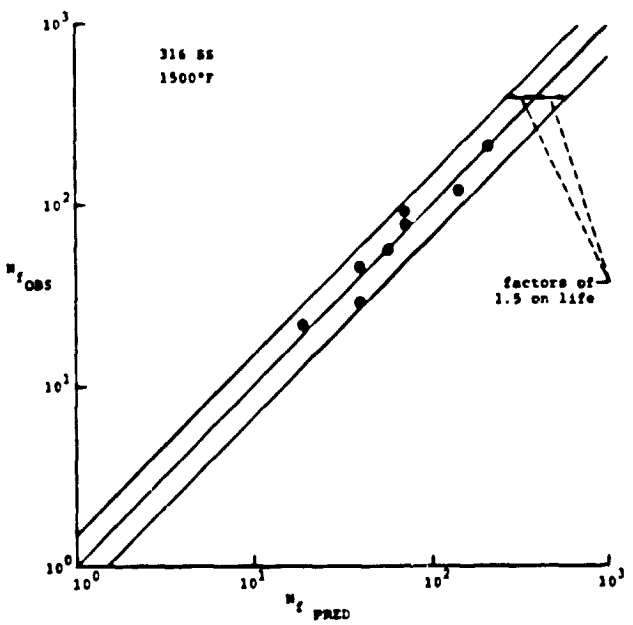

(c). N_f

Fig. 7. Comparision of Observed and Predicted Cyclic lives for CP tests with varying exposure times. Life Predictions based on Failure Time modified CP Life Relationship.

CP waveform of loading and that when it is properly accounted for, the predictions can be improved.

ii) Frequency Modified Life Equation Predictions:

Several strain rate controlled continuous cycling tests were conducted at different frequencies (thus generating varying exposure times) on 316 stainless steel at 1500°F. The results of these tests are given in Table IX. The plastic line of the Frequency Modified Life equation is generated using multiple regression analysis.

The resulting Frequency Modified Life Equation is as follows:

$$N_f = 2.9737 \left[\Delta\epsilon_{in}\right]^{-1.1709} \nu^{0.1412} \qquad (13a)$$

Frequency Modified Life:

$$N_f' = \frac{N_f}{\nu^{0.1412}} = 2.9737 \left[\Delta\epsilon_{in}\right]^{-1.1709} \qquad (13b)$$

This equation is plotted in Figure 8(a) together with the data points.

Equation (13b) is used to predict the failure lives of the CP tests with varying exposure times at 1500°F. These results are tabulated in Table X and shown in Figure 8(b). All the predicted lives are overestimated by at least a factor of 2, with many points showing a discrepancy of more than a factor of 3. This is due to the fact that Frequency Modified Life equation models a mixture of PP and CC strainranges with the frequency variation superimposed on the strainranges. Hence it cannot distinctly account for the frequency variation within the CP strainrange. For our tests the predictions were unconservative, the overprediction being as high as a factor of 5. Even higher factors of unconserva-

TABLE IX

RESULTS OF CONSTANT STRAIN RATE EXPERIMENTS
ON 316 SS AT 1500°F

Specimen No.	$\Delta\epsilon_{in}$	Frequency (cpm)	N_f
BY58	0.06741	0.01	37
BY91	0.03287	0.02	105
BY24	0.0294	0.1	161
BY30	0.00892	1	822
BY42	0.00965	0.1	484

TABLE X

LIFE PREDICTIONS OF CP TESTS WITH VARYING EXPOSURE TIMES
BY FREQUENCY MODIFIED LIFE EQUATION

Specimen	$(N_f)_{pred}$	$(N_f)_{obs}$
BY 66	583	215
BY 89	350	124
BY 87	259	94
BY 32	241	80
BY 75	187	58
BY 34	146	46
BY 96	145	29
BY 76	81	22

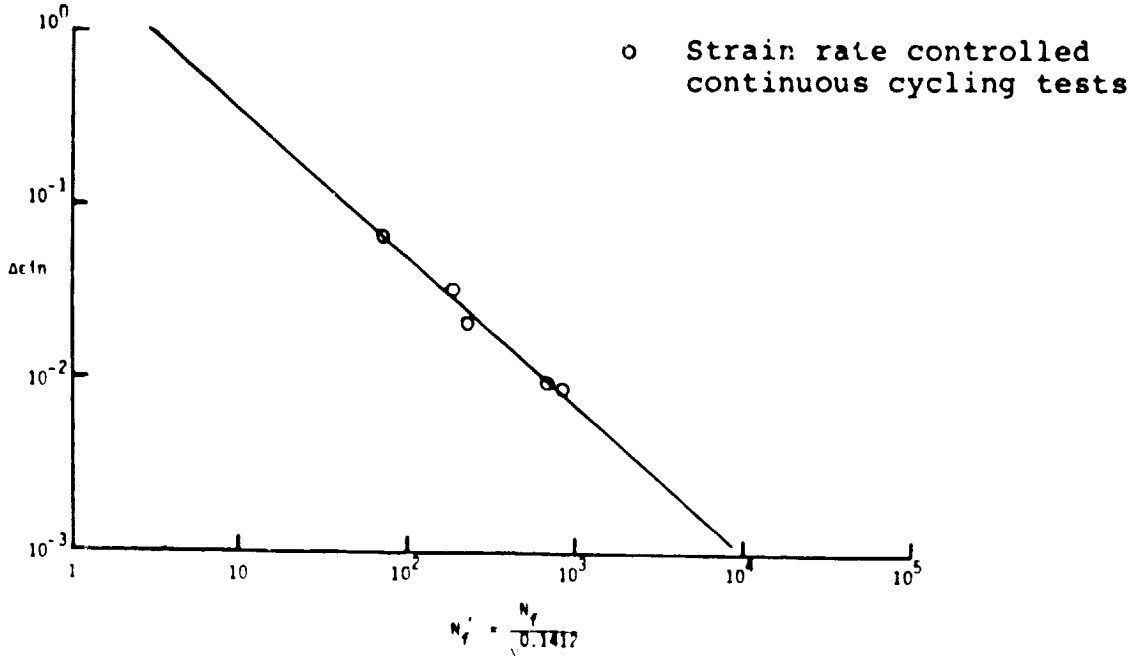

Fig. 8(a). Plastic Line of the Frequency Modified Life Equation. 316 SS at 1500° F.

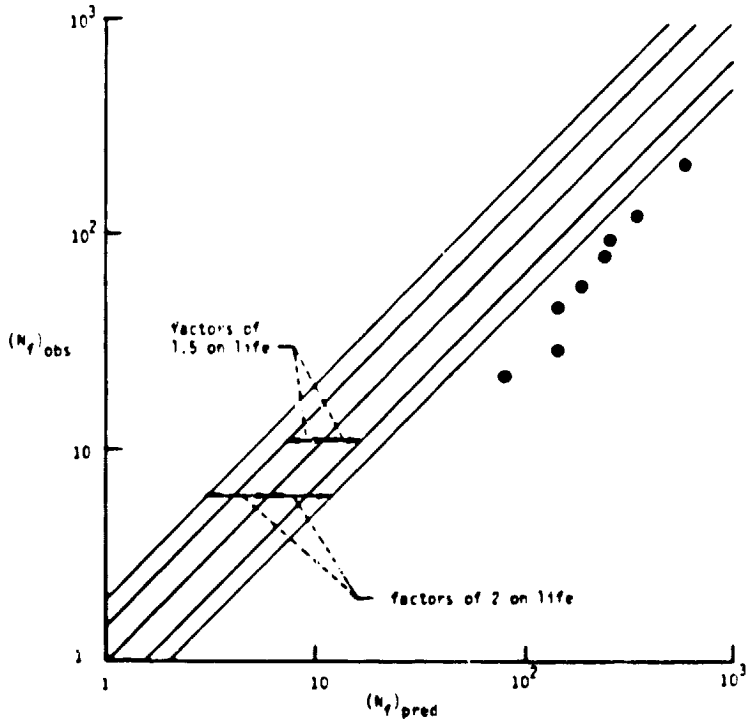

Fig. 8(b). Comparision of Observed and Predicted Cyclic lives for CP tests with varying exposure times. Life Predictions based on the Frequency Modified Life Relationship. 316 SS at 1500° F.

tiveness can be expected in other cases.

The SSCR Modified CP life relationship and the FT Modified CP life relationship account for the frequency effect within the CP strainrange. Hence they are able to predict the results within a factor of 1.5.

iii) Ductility Normalized CP Life Relationship Predictions

The creep ductility corresponding to the failure time of the constant creep strain CP test was evaluated from Eq. (9). These values were then used in conjunction with Eq. (5b) to predict the N_{cp} values. N_f predictions were obtained from these N_{cp} predictions using the Interaction Damage rule. These results are tabulated in Table XI. A plot of observed vs. predicted cyclic lives is shown in Figs. 9(a) and 9(b). In general, the life predictions are within a factor of 2. Although N_{cp} predictions follow the same trend with respect to exposure time as the experimentally observed data, the quantitative correlation is not as good as for the FT Modified CP life equation.

RESULTS OF FRACTOGRAPHY AND METALLOGRAPHY

Post-failure fractographic and metallographic investigations were conducted on four specimens of constant creep strain CP tests. Two hollow specimens at 1300°F and two solid specimens at 1500°F were selected for these investigations. The goal was to determine any micromechanistic differences between a high creep rate CP test and a low creep rate CP test (i.e. differences in the fracture modes, oxide layer formations and metallurgical aspects, etc.). The reduction in the CP generic cyclic life as the creep rate decreases can be explained using the results of fractographic and metallographic investigations.

TABLE XI

LIFE PREDICTIONS OF CP TESTS WITH VARYING EXPOSURE TIMES
BY DN-SRP LIFE EQUATIONS

Spec. No.	$\Delta\epsilon_{cp}$	tf	D_c	N_{cp} pred	N_{cp} obs	N_f pred	N_f obs
BY-66	0.01	7.95	1.792	83	105	174	215
BY-89	0.01	169.80	1.167	54	31	198	124
BY-87	0.02	3.50	2.010	29	60	49	94
BY-32	0.02	4.93	1.196	28	43	54	80
BY-75	0.02	21.44	1.559	22	24	53	58
BY-34	0.02	95.60	1.265	18	16	50	46
BY-96	0.03	2.22	2.142	16	18	26	29
BY-76	0.03	101.10	1.255	9	8	23	22

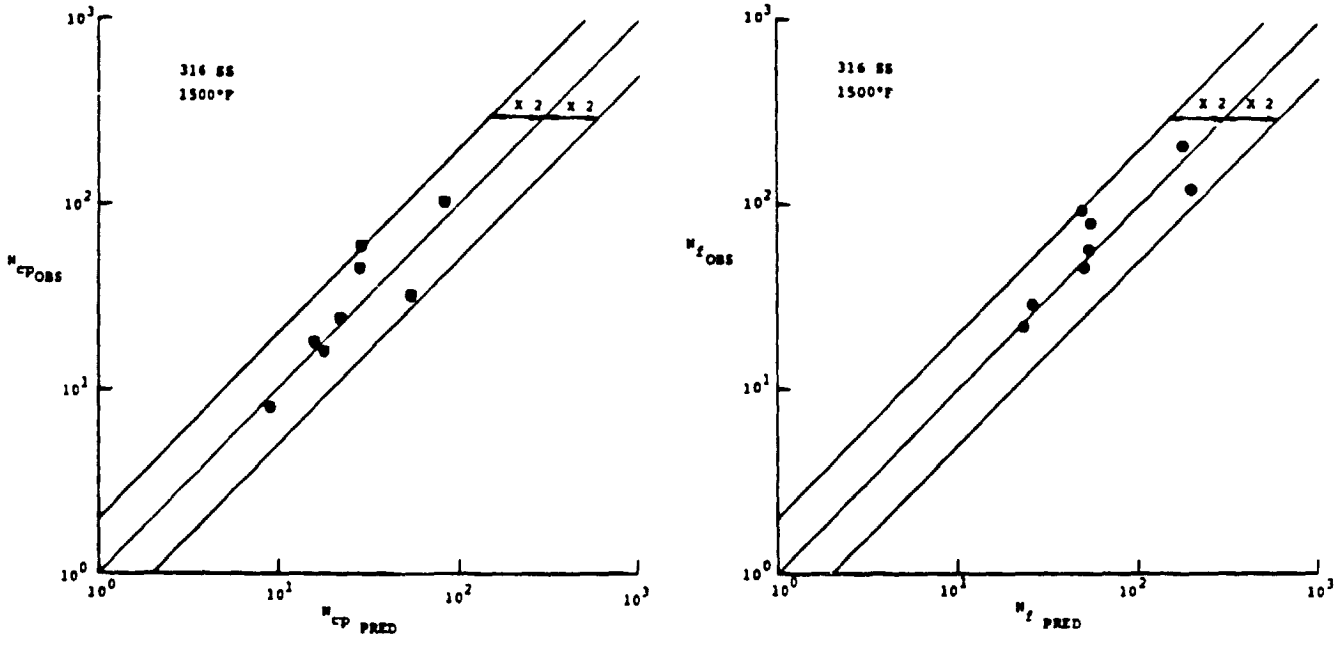

(a). N_{cp} (b). N_f

Fig. 9. Comparision of Observed and Predicted Cyclic lives for CP tests with varying exposure times. Life Predictions based on DN-SRP CP Life Relationship.

Fracture surface in a CP test resembles closely the monotonic creep fracture. Fracture occurs mainly due to the separation of grain boundaries. Grain boundary slip bands and groupings of slip bands reveal the cyclic fatigue character of CP fracture. They form from internal initiation sites very much like striations are formed from external initiation sites. These features which separate intergranular CP fatigue cracking from monotonic fracture are called 'strians' [15].

a) Fracture surface topography (high creep rate vs. low creep rate CP test)

The differences in the fracture surfaces of a high creep rate (short time duration) and a low creep rate (long time duration) constant creep strain CP tests are schematically illustrated in Fig. 10. Though both high and low creep rate tests are characterized by intergranular fracture, the severity of intergranular fracture, microvoid formation and oxidation are different in these two cases.

The salient features of the fracture surfaces of a high creep rate and low creep rate constant creep strain CP tests are as follows:

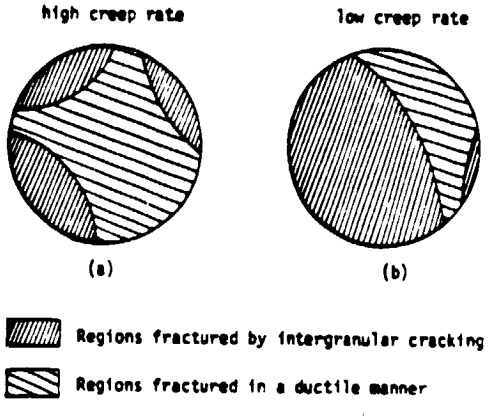

Fig. 10. Schematic Illustration of fracture surface appearances in (a) high creep rate and (b) low creep rate constant creep strain CP tests.

Feature	Fast creep rate	Slow creep rate
1) Number of crack initiation sites at the surface of the specimen	Large number	A single dominant crack with few initiation sites
2) Intergranular fracture	Several small regions	Large areas of severe IG cracking
3) Ductile fracture	Large region	Small region
4) Density of grain boundary strian markings	High	Low
5) Microvoids at internal sites	Relatively few	Many microvoids showing agglomeration into a huge void
6) Fracture surface	Relatively clean because little time is allowed for oxidation of the surface	Heavily oxidized. Oxide can sometimes mask the details of fracture surface topography.

The SEM photomicrographs illustrating the above features are presented in Figures 11(a) to 11(d). Multiple crack initiation sites and transition from intergranular fracture to ductile fracture occurring in a high creep rate CP test are shown in Fig. 11(a). Typical intergranular fracture and microvoid formation at internal sites in a low creep rate CP test are illustrated in Fig. 11(b). These tests were conducted on solid specimens of 316 SS at 1500°F. Similar photomicrographs for tests conducted on hollow specimens of 316 SS at 1300°F are presented in Figs. 11(c) and 11(d). The features observed at 1300°F are similar to those observed at 1500°F. Intergranular fracture with high strian

(a). High Creep rate test

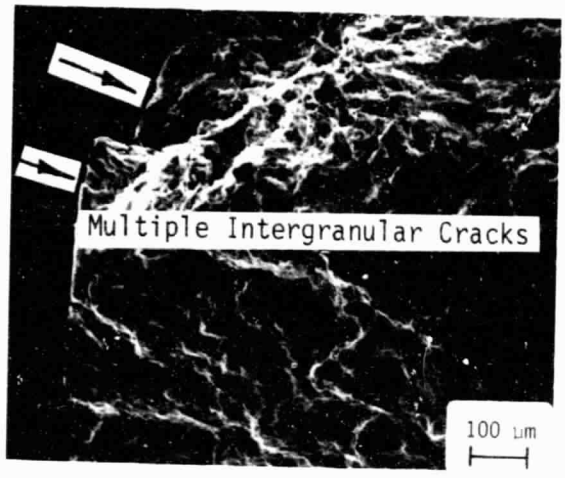

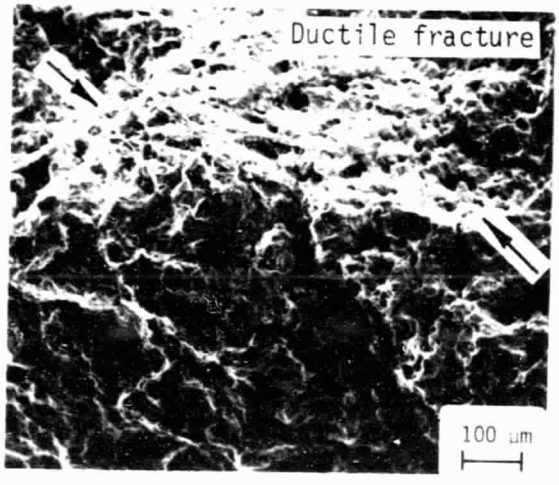

$\dot{\varepsilon}_{ss}$ = 0.004024 in/in/min

N_f = 94

t_f = 3.5 hr

(b). Low Creep rate test

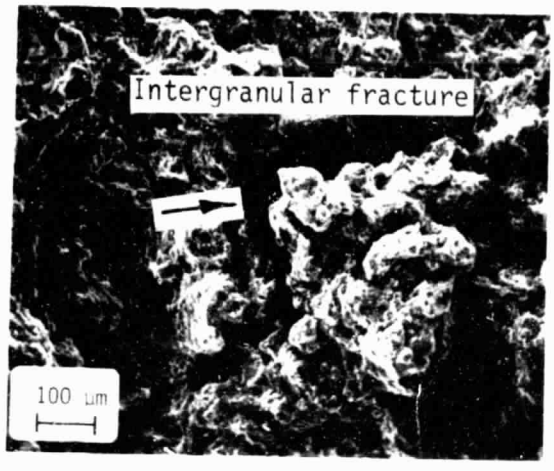

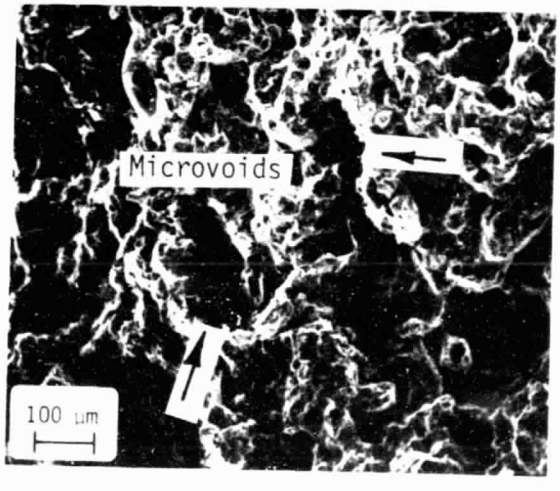

$\dot{\varepsilon}_{ss}$ = 0.0000338 in/in/min

N_f = 46

t_f = 95.60 hr

Fig. 11. Comparision of the Fracture Surface Topography of a High Creep rate test and a Low Creep rate test. 316 SS at 1500° F. $\Delta\varepsilon_{in}$ = 2%.

(c). High Creep rate test

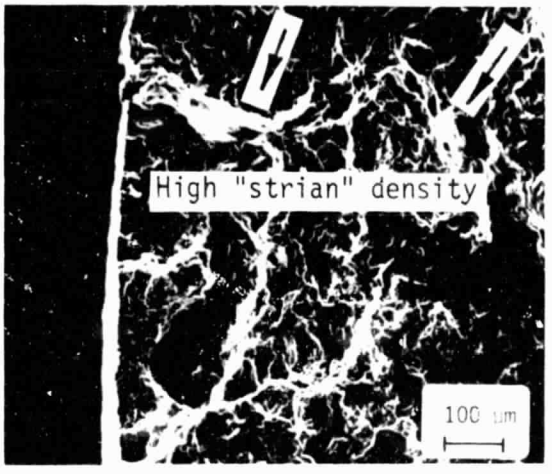

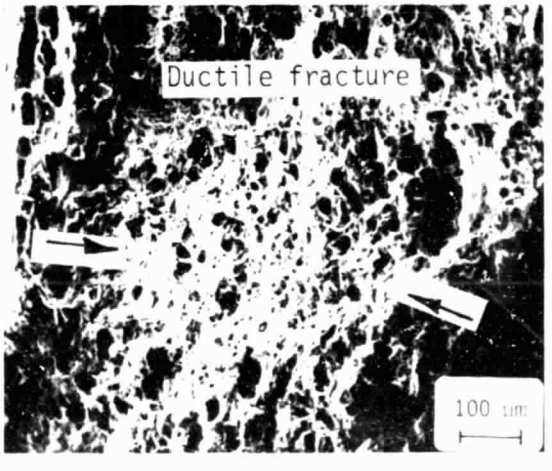

$\dot{\varepsilon}_{ss}$ = 0.0006062 in/in/min

N_f = 69

t_f = 10.1 hr

(d). Low Creep rate test

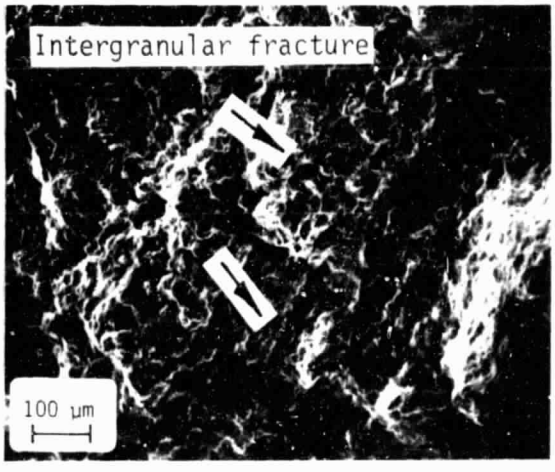

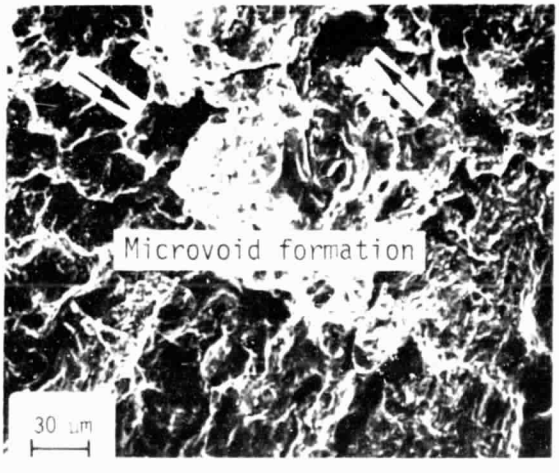

$\dot{\varepsilon}_{ss}$ = 0.0000430 in/in/min

N_f = 45

t_f = 142.3 hr

Fig. 11 (Continued) 316 SS at 1300° F, $\Delta\varepsilon_{in}$ = 2%

density in a high creep rate constant creep strain CP test is visible in Fig. 11(c).

Macrophotographs of the metallographic sections of high creep rate and low creep rate constant creep strain CP tests are illustrated in Figs. 12(a) and 12(b), respectively. Two separate crack initiation sites on the surface of a high creep rate CP test specimen are clearly visible in Fig. 12(a). The material between the two crack fronts fractured in a ductile manner. The intergranular nature of fracture is distinctly visible in Fig. 12(b). It appears that crack propagation occurs in a low creep rate CP test by means of linking the microvoids and intergranular cracking formed ahead of crack tip within the bulk of the material. Thus the crack is propagated along a path that is already weakened by microvoids and intergranular cracks. Multiple crack initiation sites developed at the surface of a specimen in a high creep rate CP test and a huge void formed during a low creep rate CP test can be seen in Figures 13(a) and 13(b), respectively.

b) Oxide Formation

The formation of an oxide layer on the surface and within the crevice of the crack can influence the crack growth rate and hence the cyclic life of a constant creep strain CP test. During the rapid compressive loading in a CP cycle the oxide gets "wedged" between the two lips of the crack. This can either sharpen the crack tip to a greater extent or possibly propagate the crack during compression, if sufficiently thick oxide layer is available. A schematic of the oxide wedging effect mechanism is shown in Fig. 14. Photomicrographs of the high creep rate and low creep rate CP test specimens were obtained using an optical microscope prior to etching to preserve the oxide layers. These photomicro-

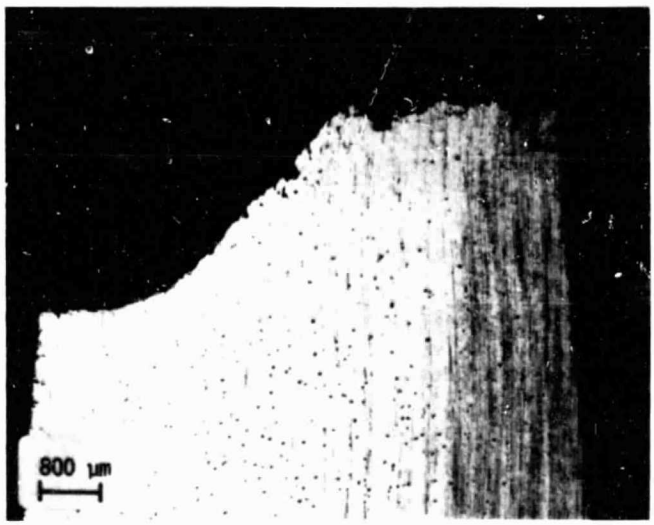

(a). High Creep rate test

$\dot{\varepsilon}_{ss}$ = 0.004024 in/in/min; N_f = 94; t_f = 3.5 hr.

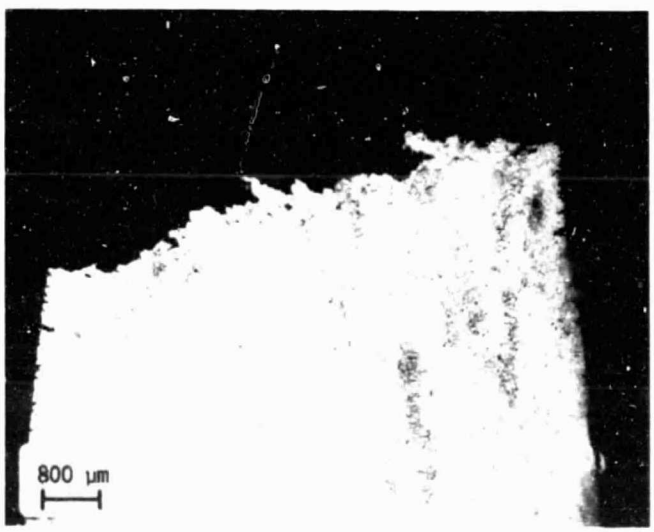

(b). Low Creep rate test

$\dot{\varepsilon}_{ss}$ = 0.0000338 in/in/min; N_f = 46; t_f = 95.6 hr.

Fig. 12. Metallographs of specimens fatigued to failure in CP tests with varying exposure times. 316 SS at 1500° F. $\Delta\varepsilon_{in}$ = 2%.

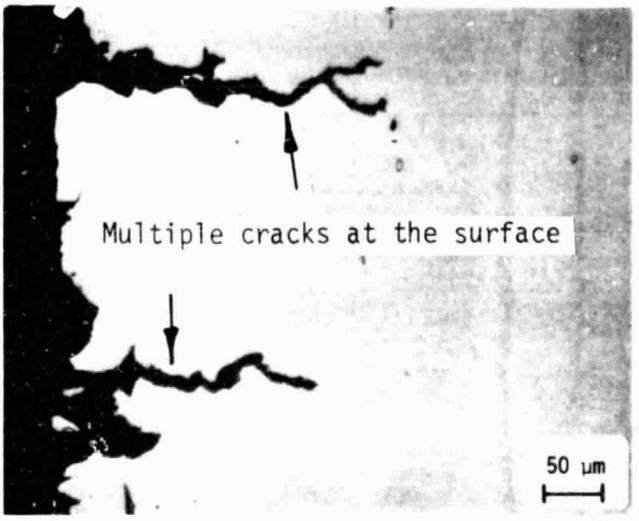

(a). High Creep rate test

$\dot{\varepsilon}_{ss}$ = 0.004024 in/in/min; N_f = 94; t_f = 3.5 hr.

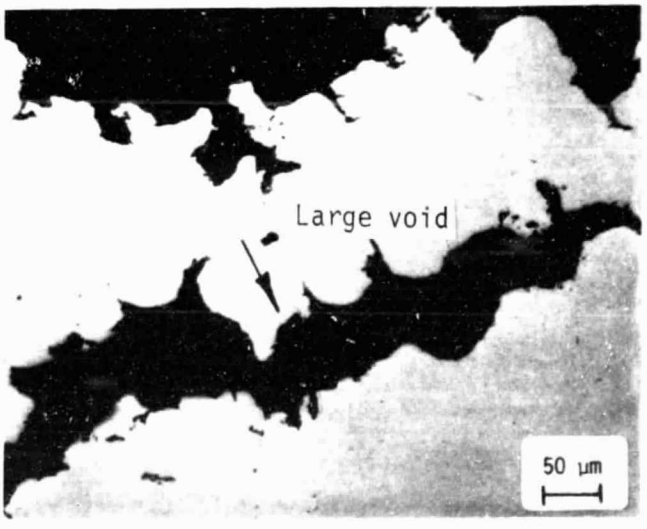

(b). Low Creep rate test

$\dot{\varepsilon}_{ss}$ = 0.0000338 in/in/min; N_f = 46; t_f = 95.6 hr.

Fig. 13. Typical Features of High Creep rate and Low Creep rate CP tests with varying exposure times. 316 SS at 1500° F. $\Delta\varepsilon_{in}$ = 2%.

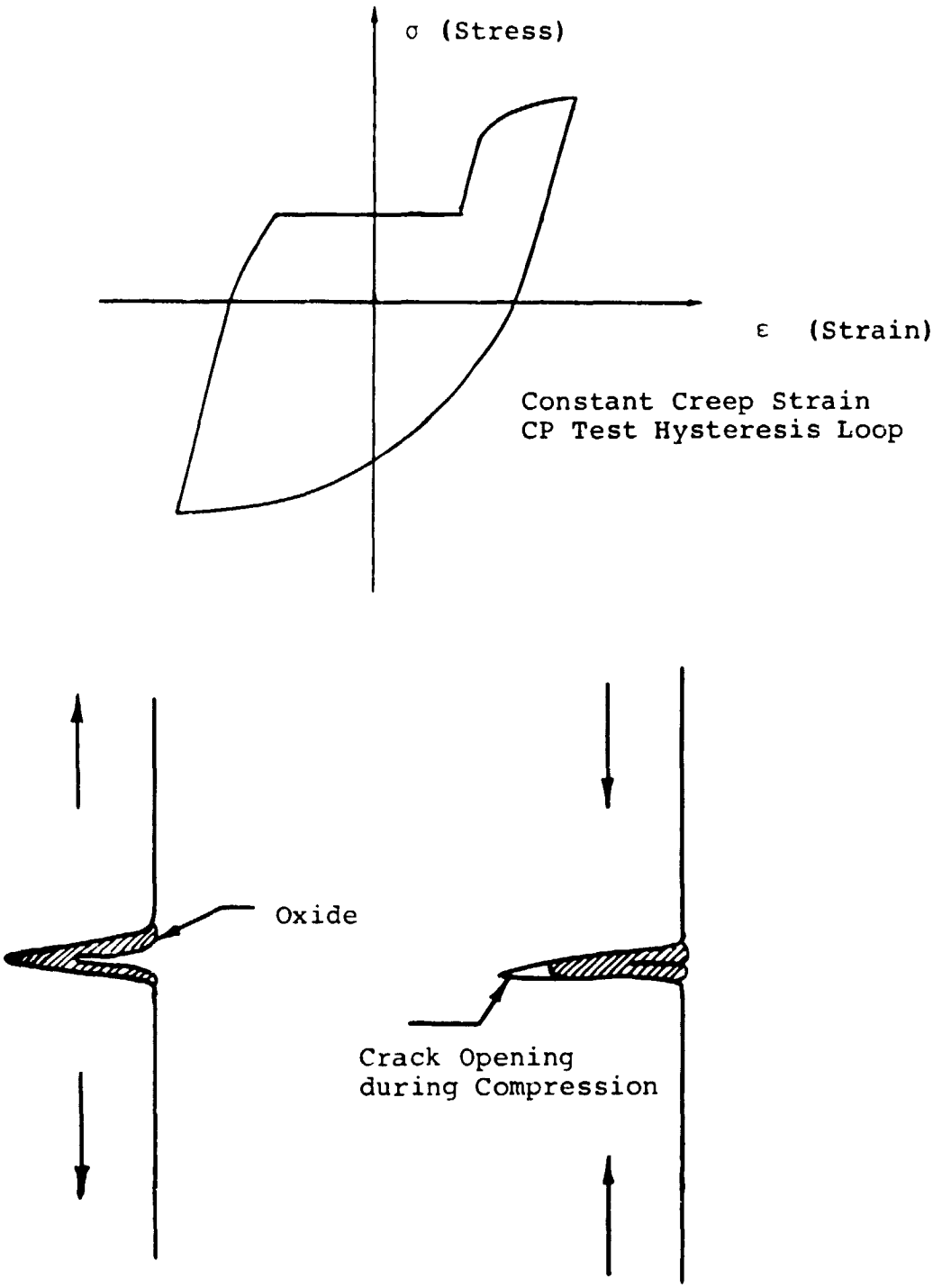

Fig. 14. Oxide Wedge Effect.

graphs are illustrated in Figures 15(a) to 15(d). The grey colored regions indicate the oxide layers. It is clear from these figures that the longer the failure time (or lower the creep rate), the greater the thickness of the oxide layer. Also at high temperature (1500°F, Figs. 15(a) and 15(b)), the oxide layer is thicker than at a lower temperature (1300°F, Figs. 15(c) and 15(d). An oxide wedging effect is more likely to be observed when the oxide layer is thick than when it is thin. In a slow creep rate CP test there is sufficient time for the oxide layer to form and develop into a thicker layer as compared to a high creep rate CP test. Hence, oxide wedge effect is possibly one reason why a lower cyclic life is observed in a low creep rate CP test as compared to a high creep rate CP test.

c) Metallurgical Instabilities in Austenitic Steels

AISI 316 stainless steel is an austenitic steel with chromium and nickel as the major alloying elements. Unless the carbon content is very low (i.e. < 0.02%), the homogeneous structure of stainless steel (after annealing between 1850° and 2050°F) is the result of quasi-equilibrium. Carbon is held in the solution due to rapid cooling caused by quenching. When austenitic stainless steels are reheated between 900° to 1700°F, the carbon in the supersaturated solution is rejected and the resulting carbides alter the properties of steel. Sensitization to intergranular corrosion and changes in mechanical properties are two direct consequences resulting from the precipitation of carbides. These carbides are usually of the form $M_{23}C_6$ where M denotes any metal. $M_{23}C_6$ is usually made up of chromium carbide in which iron (or molybdenum) may substitute partially for chromium.

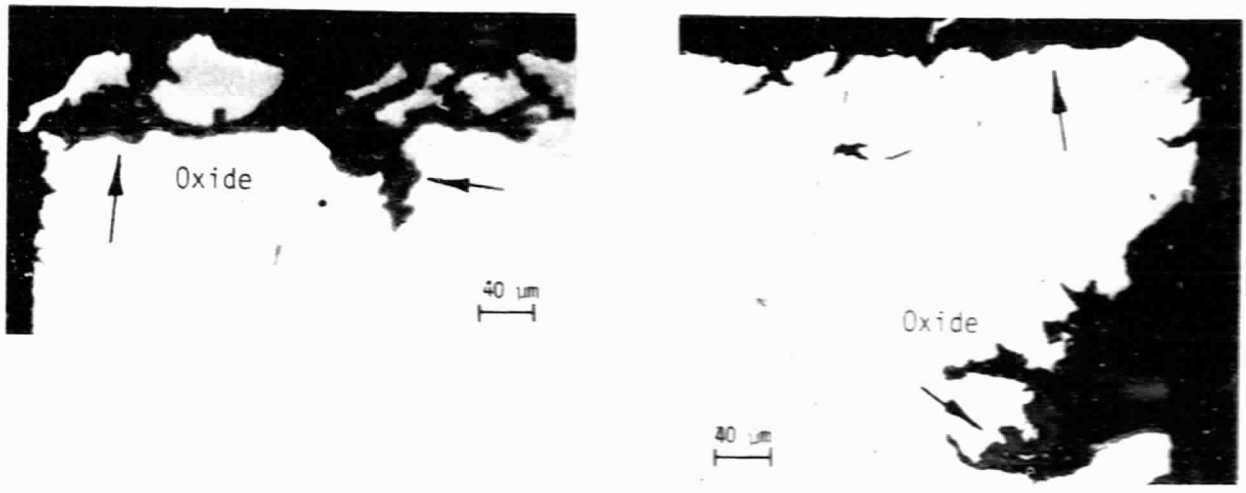

(a). High Creep rate test

$\dot{\varepsilon}_{ss}$ = 0.004024 in/in/min; N_f = 94; t_f = 3.5 hr.

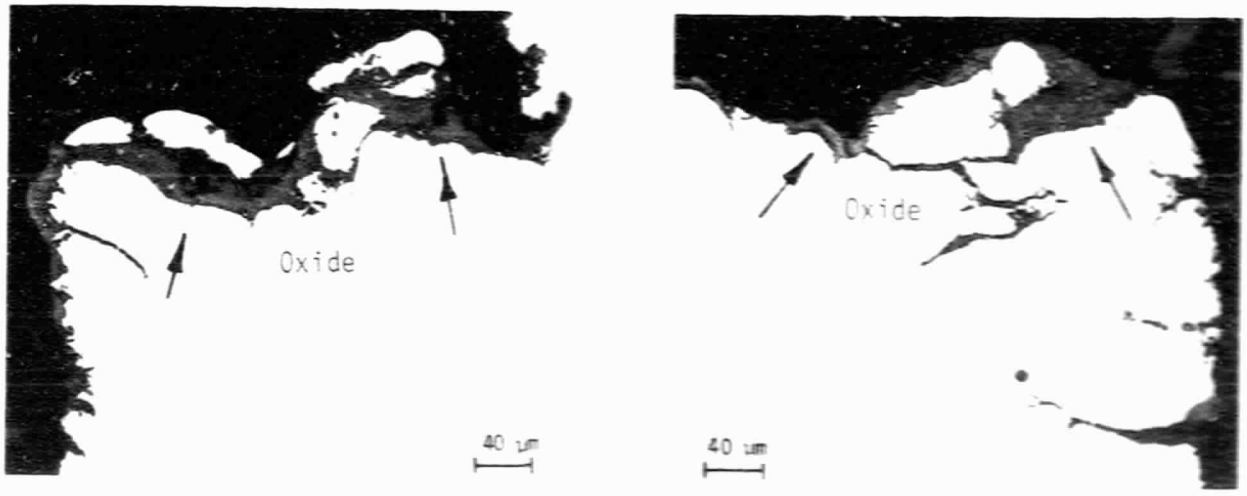

(b). Low Creep rate test

$\dot{\varepsilon}_{ss}$ = 0.0000338 in/in/min; N_f = 46; t_f = 95.6 hr.

Fig. 15. Oxide Layer Formation in CP tests with varying exposure times. 316 SS at 1500° F. $\Delta\varepsilon_{in}$ = 2%.

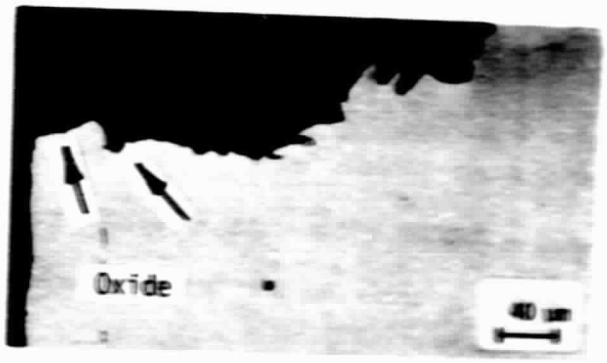

(c). High Creep rate test

$\dot{\epsilon}_{ss}$ = 0.0006062 in/in/min; N_f = 69; t_f = 10.1 hr

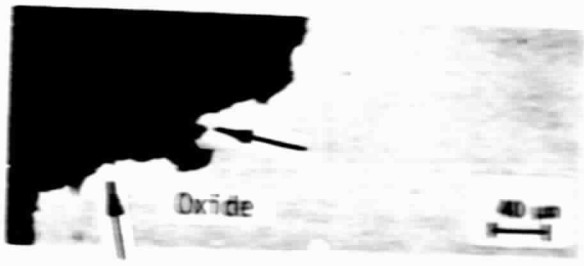

(d). Low Creep rate test

$\dot{\epsilon}_{ss}$ = 0.00043 in/in/min; N_f = 45; t_f = 142.3 hr

Fig. 15 (Continued) 316 SS at 1300° F. $\Delta\epsilon_{at}$ = 2%.

Statistically, the precipitation of chromium carbide is favored along the grain boundaries, though precipitations can also occur at slip bands and around non-metallic inclusions. The carbon atom being small diffuses more rapidly through the austenitic crystal than chromium which is a bigger atom. As a result, during the process of precipitation, carbon atoms migrate to the grain boundary from all parts of the crystal, whereas chromium is depleted from more localized regions, near the grain boundary, thus creating an envelope of chromium-depleted material in the vicinity of grain boundary. A schematic of this mechanism is illustrated in Fig. 16. Hence, the chromium-depleted grain boundaries are susceptible to corrosion and fracture. In addition, the galvanic effect arising between the precipitated chromium carbide particles and the austenite matrix can accelerate the corrosion. At a given temperature the amount of chromium carbide increases with the time of exposure.

The metallographic sections of the specimens fatigued to failure in constant creep strain CP tests were etched [1] and photographed using the scanning electron microscope. Figures 17(a) and (b) show the results of a high creep rate CP test and low creep rate CP test, respectively, at 1500°F. Figures 17(c) and (d) show corresponding results for tests conducted at 1300°F. The short time test (Fig. 17(a)) practically has no precipitation of chromium carbide along the grain boundaries compared to the long time test (Fig. 17(b)) which shows oxidized microvoids and separation of grain boundaries in regions far away from

[1] Composition of the etchant used: (Proposed by Marble)
4 grams of copper sulphate
20 cc of hydrochloric acid
20 cc of water

Original Microstructure

Annealed at 1850-2050° F

Reheated to 900-1700° F

+ Hold Period

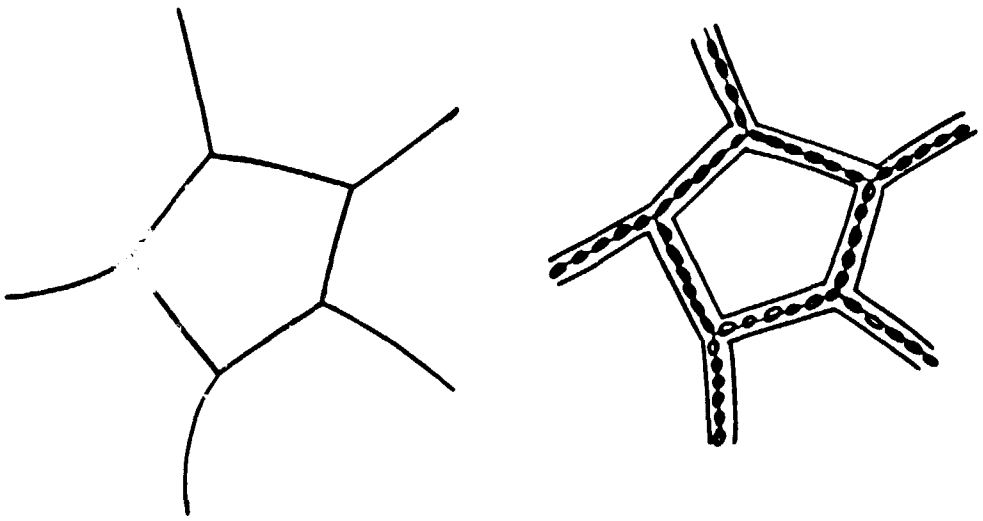

Chromium Carbide Precipitation

Chromium Depleted Zone

Fig. 16. Austenitic Stainless Steel (C > 0.02%)
Schematic Illustration of Sensitization.

(a). High Creep rate test

(b). Low Creep rate test

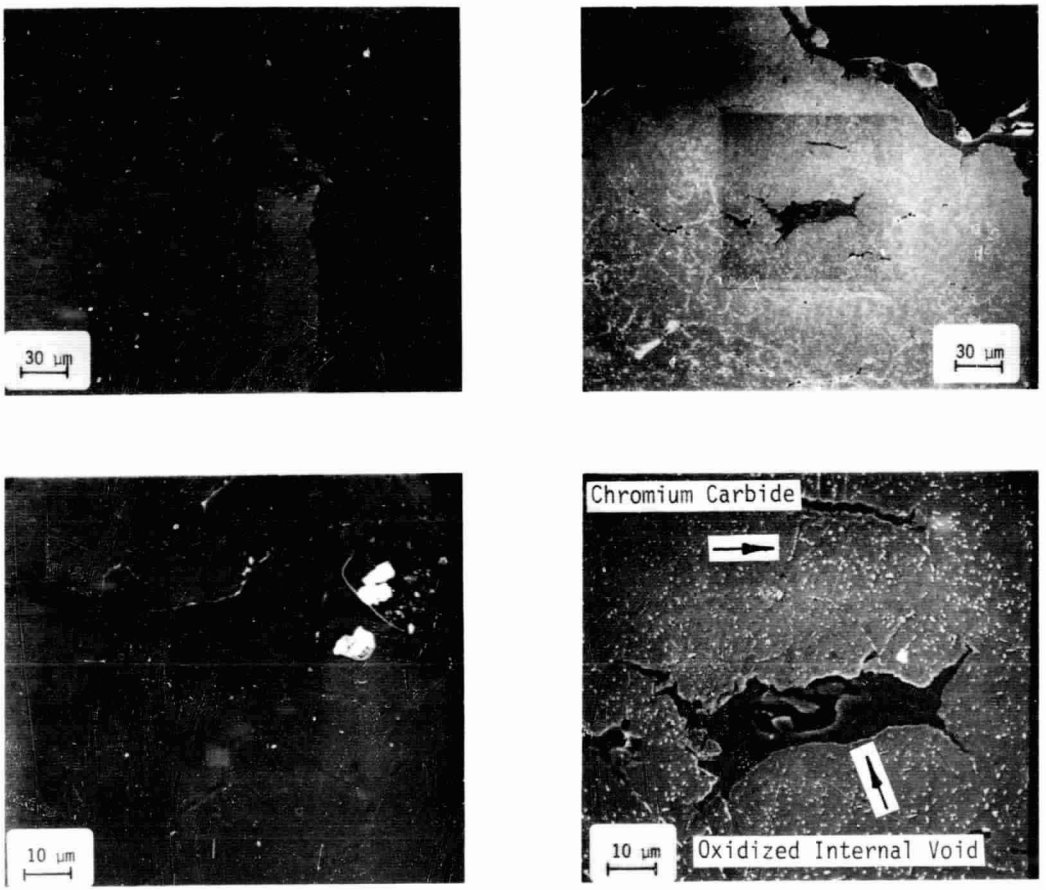

$\dot{\varepsilon}_{ss}$ = 0.004024 in/in/min

N_f = 94

t_f = 3.5 hr

$\dot{\varepsilon}_{ss}$ = 0.0000338 in/in/min

N_f = 46

t_f = 95.60 hr

Fig. 17. Comparision of the Metallographic sections of specimens fatigued to failure in CP tests with varying exposure times. 316 SS at 1500° F. $\Delta\varepsilon_{in}$ = 2%.

the actual fracture surface. Comparing Figs. 17(c) and 17(d), it can be seen that more chromium carbide precipitation is present in the long time duration test than in the short time duration test. In addition, Fig. 17(d) illustrates intergranular fracture that developed within the bulk volume of the material during a long time duration test.

Since carbide precipitation makes the grain boundaries susceptible to fracture (i.e. more brittle) and the amount of carbides precipitating increases with the time at a given temperature, the grain boundaries are more vulnerable in long time duration CP tests. This is one reason why lower cyclic life is observed in long exposure time constant creep strain CP tests.

DISCUSSION

Time effects on N_{cp} have been treated in this report according to two types of equations. Both of these equations are reproduced below for convenience. The first type, namely the Steady State Creep Rate (SSCR) Modified CP life equation,

$$N_{cp} = A \left[\Delta\epsilon_{cp}\right]^{\alpha} \left[\dot{\epsilon}_{ss}\right]^{\beta} \qquad (11a)$$

is reminiscent of Coffin's Frequency Modified Life equation (FML). However, the nature of the terms involved in this equation differ considerably from those in the FML equation. As discussed more fully earlier in the report, the FML equation reflects both a creep rate effect and a rheological effect wherein the ratio of CC to PP strain changes as frequency is changed. Thus there would be an apparent "time" effect even if no metallurgical phenomena were introduced by longer exposure, just because in the lower frequency tests a larger content of

(c). High Creep rate test

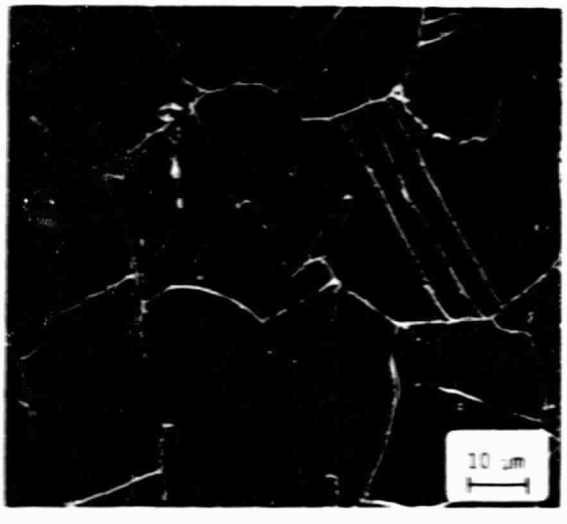

$\dot{\varepsilon}_{ss}$ = 0.0006062 in/in/min

N_f = 69

t_f = 10.1 hr

(d). Low Creep rate test

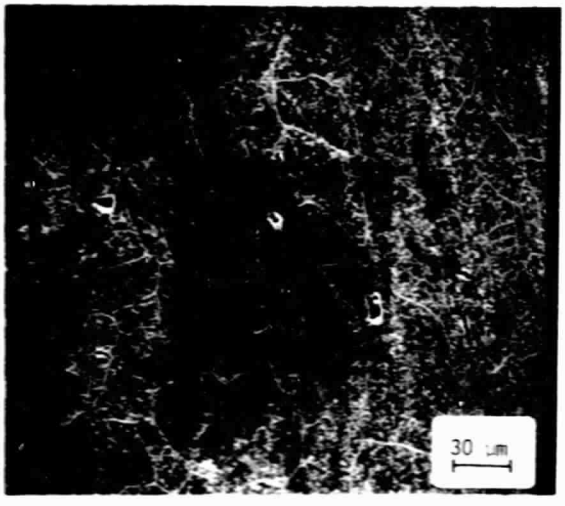

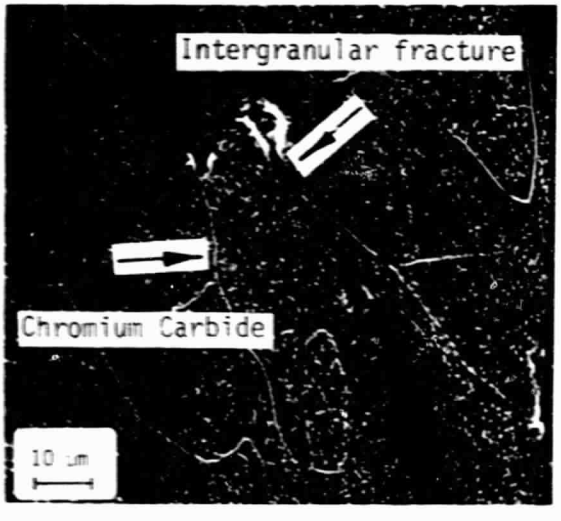

$\dot{\varepsilon}_{ss}$ = 0.000043 in/in/min

N_f = 45

t_f = 142.3 hr

Fig. 17 (continued) 316 SS at 1300° F. $\Delta\varepsilon_{in}$ = 2%.

the imposed strainrange becomes the CC type which is more damaging than the PP type. Furthermore such "time" effects as are observed refer to effects on the CC type of strainrange, and not on the CP type investigated in this study. Extrapolations to lower creep rates by the FML equation would therefore not carry the same fundamental implications regarding N_{cp} as those determined from Eq. (11a).

The second form of the equation, namely, the Failure Time (FT) Modified CP life equation

$$N_{cp} = B \left[\Delta \epsilon_{cp}\right]^{\gamma} \left[t_f\right]^{\delta} \qquad (12a)$$

would seem to bear a closer relation to the Ductility Modified approach that has been used in the past to correct N_{cp} life for materials with ductilities in the extrapolation range which are different from those in the testing range. In fact, if ductility can be expressed as a power law of rupture time, it is clear that the two approaches could ideally produce identical results. Eq. (12a) would seem, however, to be more direct, and probably more accurate for moderate extrapolations of rupture times. For very long extrapolations, the favor might revert to the Ductility Modified equation approach, since actual ductilities for very long times (say 10^5 hrs.) might be available from creep-rupture tests while Eq. (12a) reflects ductility variation in only the experimental range for the cycling tests. Thus, if a material develops a metallurgical instability (say the precipitation of a sigma phase) after 10,000 hrs., the creep rupture tests, although they are static, are more likely to reveal this development more accurately than a shorter time fatigue test. Since static creep-rupture tests on many materials are more plentiful than creep-fatigue tests, use of ductility information revealed by

these tests should not be overlooked, even though equations of the form (12a) may give more accurate results in the creep-fatigue experimental range. For the tests of this investigation, for example, Eq. (12a) gave correlations within a factor of 1.5 on life in the experimental range while the Ductility-Modified approach gave results within a factor of 2.0. However, if long-time ductility in creep-rupture tests are available their implications for long-time extrapolation of creep-fatigue tests should not be overlooked. It should also be recognized, of course, that if ductility degrades in an abrupt manner only after long time exposure, the creep-fatigue analysis must proceed on a cycle-by-cycle basis reflecting in each applied cycle only the damage that is developed for a cycle within the material at its current ductility. This subject has been discussed in Ref. (6,19).

Although both forms of the equations (11a) and (12a) give approximately the same degree of accuracy in the experimental range used in this investigation, it should not be inferred, of course, that both forms are identical. Obviously, since the exponents on $\Delta\epsilon_{cp}$ are different, computed lives by each of the two equations must be at least slightly different even if a relation between rupture time and creep rate exists. Thus, although it is possible that the $\left[\dot{\epsilon}_{ss}\right]^{\beta}$ in Eq. (11a), and the $\left[t_f\right]^{\delta}$ in Eq. (12a) are inter-related and yield the same mathematical information, the fact that α is not equal to γ indicates that the two equations will not always yield the same life value. Which type of equation is more useful for extrapolation requires further study.

It should also be pointed out that the time (or creep-rate) effect on the CP life relation was obtained by assuming that the PP life relation was not time-dependent. When only PP cycles are applied a time-dependency need not be considered, since in principle a very large number of cycles can be applied in a

very short time. However, when, in effect, the PP cycles are applied concurrently with the CP cycles, the PP cycles are also applied as the material is degrading while the material interacts with the environment and degrades metallurgically. Thus it is possible that some consideration should be given to N_{pp} degradation with time, which might change the result of these tests to some extent.

In this investigation we have considered only the CP type of strainrange. It is clear that for complete SRP analyses involving other types of strainranges, similar studies are required for PC, CC and even PP, as mentioned above. For evaluations of time effects on PC lives, the approach used in this study can be used in a similar manner, but for CC evaluations there are two independent variables -- the creep rate in tension and the creep rate in compression. The time effects on CC strainranges will therefore require additional consideration in order to minimize the extent of the testing program involved.

A final point that must be considered for future programs on any of the types of strainranges associated with the SRP framework. When an imposed loop contains more than one strainrange, the experimental information obtained provides information only on life for each type of strainrange for a magnitude equal to the total strainrange of the loop. Thus, for example, if the total strainrange is 1% and consists of a CP strainrange of 0.5% and PP strainrange of 0.5%, the test involves information on N_{pp} and N_{cp} for $\Delta\epsilon_{pp}$ = 1% and $\Delta\epsilon_{cp}$ = 1%. If the test were changed so that the imposed 1% total strainrange consisted of 0.75% CP and 0.25% PP, the information involved in the test still only involves N_{pp} and N_{cp} for a strainrange of 1%. This is a peculiarity of the Interaction Damage Rule. Thus, to get information on N_{cp} at a strainrange of 2%, the loop used must have a total strainrange of 2%, and it doesn't matter whether 0.5%

or 1%, or 1.5% of this loop consists of CP strainrange. Obviously, however, the larger the fraction of the total strainrange that is imposed as CP, the more accurate will be the information on the life N_{cp} at the strainrange of 2%. In the tests conducted in this program the PP component was included for convenience of programming to maintain constant total strainranges even though some variation in CP strainrange inevitably occurred. However, it would seem that in future tests the control system should be improved to minimize the amount of PP needed, and to keep the CP (or other components, when they are studied) at the largest fraction of the total strainrange practicable.

SUMMARY AND CONCLUDING REMARKS

The effect of creep rate (or exposure time) within the CP strainrange (or waveform) was investigated by conducting a series of CP tests with varying creep rates (or exposure times) on 316 SS at 1300°F and 1500°F. A reduction in N_{cp} lives was observed with a reduction in the creep rate (or with an increase in the exposure time).

The reasons for the reduction of cyclic life as creep rate decreases are summarized below:

1. In the case of a low creep rate test, cracks propagate by linking the microvoids and minute cracks caused by grain boundary separation, i.e., they propagate along a path that is already weakened by microvoids and intergranular cracks. In a high creep rate test since sufficient time is not allowed for microvoid formation, crack propagation requires physical separation of grain boundaries. Hence the crack growth rate $\left[\frac{da}{dN}\right]$ in the case of low creep rate test is likely to be much higher than the one in the high creep rate test.

2. Oxide layers within the crack crevices of a specimen can accelerate the crack growth rate due to an oxide wedge effect. A low creep rate test allows sufficient time for the build-up of oxide layers and hence the wedge effect can reduce the cyclic life of a low creep rate test more than a high creep rate test.

3. The sensitization of austenitic stainless steel, due to the precipitation of chromium carbide along the grain boundaries, can make the steel more susceptible to intergranular corrosion. Hence a long time duration test (low creep rate) is more damaging than a short time duration test (high creep rate).

The reduction in cyclic life with a reduction in creep rate is a combined effect of micromechanistic damages occurring in the material due to low creep rates and due to environmental effets such as oxidation, corrosion, etc. In order to separate the damage associated with the material's rheological behavior from the damage caused to the material by the environment, similar tests should be conducted in vacuum or an inert atmosphere.

The Ductility-Normalized SRP life relationships can also be used to account for the reduction in cyclic life with an increase in the failure time but not with the same accuracy as was obtained with the new relations. The predictions of DN-SRP life relationships were generally within a factor of 2. When no cyclic creep fatigue data are available DN-SRP relations satisfactorily predict lives.

The conventional Strainrange Partitioning method predicted the lives within a factor of 2. However, conventional SRP does not account for frequency effects within a given type of strainrange. The Steady State Creep Rate (SSCR) Modified CP life relationship and the Failure Time (FT) Modified CP life relationship predicted the lives within a factor of 1.5. Thus life predictions can be improved by accounting for the effect of frequency and waveform in a distinct manner. It is also necessary to account for exposure time (or creep rate) when the creep

fatigue data generated at short times are being extrapolated to longer times.

As illustrated in the discussion section, there is a difference between the SSCR Modified CP life relationship and the FT Modified CP life relationship. The question as to which one of these two equations is more appropriate depends upon the circumstances. In the future more experiments should be conducted on a wide spectrum of materials to resolve this issue. The present work provides a good format for such future investigations.

ACKNOWLEDGMENTS

The authors gratefully acknowledge the financial support (Grant Number: NAG3-337, Dr. G. R. Halford, Grant Monitor) provided by NASA-Lewis Research Center, Cleveland, Ohio.

REFERENCES

1. Manson, S.S., G.R. Halford and M.H. Hirschberg: "Creep-fatigue analysis by strain-range partitioning," NASA TM X-67838, Technical paper presented at Pressure Vessels and Piping Conference sponsored by the American Society of Mechanical Engineers, San Francisco, California, May 10-12, 1971.

2. Halford, G.R., J.F. Saltsman and M.H. Hirschberg: "Ductility-Normalized Strainrange Partitioning Life Relations forCreep-Fatigue Life Predictions" - NASA TM-73737, Technical paper presented at the Conference on Environmental Effects and Degradation of Engineering Materials, sponsored by the Virginia Polytechnic Institute, Blacksburg, Virginia, October 10-12, 1977.

3. Kalluri, S., "The effect of creep rate on Strainrange Partitioning life relationships," M.S. Thesis, Department of Mechanical and Aerospace Engineering, Case Western Reserve University, January, 1984.

4. Manson, S.S., G.R. Halford and A.J. Nachtigall: "Separation of the strain components for use in strainrange partitioning," NASA TM X-71737, Technical paper presented at Pressure Vessels and Piping Conference, sponsored by The American Society of Mechanical Engineers, San Francisco, California, June 23-27, 1975.

5. Hirschberg, M.H.: "A Low Cycle Fatigue Testing Facility," Manual on low cycle fatigue testing, ASTM STP 465, American Society for Testing Materials, 1969, pp 67-86.

6. Coffin, L.F, Jr., A.E. Carden, S.S. Manson, L.K. Severud and W.L. Greenstreet: "Time-Dependent Fatigue of Structural Alloys, A General Assessment" (1975), prepared by the Oakridge National Laboratory, Oakridge, Tennessee, January 1977, pp 37-332.

7. Manson, S.S.: "The Challenge to Unify Treatment of High Temperature Fatigue - A Partisan Proposal Based on Strainrange Partitioning," Fatigue at Elevated Temperatures, ASTM STP 520, American Society for Testing and Materials, 1973, pp 744-782.

8. Manson, S.S. and G.R. Halford: "Complexities of High Temperature Metal Fatigue - Some Steps Toward Understanding," Technical paper presented at The Twenty-fifth Annual Israeli Conference on Aeronautics and Astronautics sponsored by the University of Haifa, Haifa, Israel, February 23-25, 1983. NASA TM 83507.

9. Halford, G.R., A.J. Nachtigall: "The Strainrange Partitioning Behavior of an Advanced Gas Turbine Disk Alloy, AF2-1DA" AIAA/SAE/ASME 15th Joint Propulsion Conference, June 18-20, 1979, Las Vegas, Nevada, pp. 4-8.

10. Manson, S.S., G.R. Halford and R.E. Oldrieve: "Relation of Cyclic Loading Pattern to Microstructural Fracture in Creep-Fatigue," Proceedings, The

Second International Conference on Fatigue and Fatigue Thresholds. Birmingham, 1984. C.J. Beevers Ed., Engineering Materials Advisory Services Ltd., West Midlands, U-K, 1984.

11. Parr, J.G. and A. Hanson, "An Introduction to Stainless Steel." American Society for Metals, 1965, pp. 52-56.

12. Colombier, L. and J. Hockmann: "Stainless and Heat Resisting Steels." Edward Arnold (publishers) Ltd., 1967, pp. 84-93.

13. Peckner, D. and I.M. Bernstein: "Handbook of Stainless Steels." McGraw-Hill Book Company, 1977, pp. 4-35 to 4-52.

14. Williams, R.S. and V.O. Homeberg: "Principles of Metallography." Third edition, McGraw-Hill Book Company, Inc.

15. Oldrieve, R.E.: "Fractographic Evaluation of Creep Effects on Strain Controlled Fatigue Cracking of AISI 304 LC and 316 Stainless Steel." NASA TM-78913, Lewis Research Center, Cleveland, Ohio, June 1978.

16. Rostoker, W. and J.R. Dvorak: "Interpretation of Metallographic Structures." Second edition, 1977, Academic Press Inc., pp. 66-74.

17. "MTS Basic RT-11 Users Guide." MTS Systems Corporation, November 1976.

18. "MTS Basic Assembly Language Routines Program Manual." MTS Systems Corporation, July 1977.

19. S. S. Manson and R. Zab: "Treatment of Low Strains and Long Hold Times in High Temperature Metal Fatigue by Strainrange Partitioning." ORNL/Sub-3988/1 August, 1977.

APPENDIX A

CONCP.BAS Program Listing

```
CONCP       MTS BASIC V01B-02C

100 PRINT " THIS PROGRAM RUNS A CONSTANT CREEP 'CP' TEST "
110 REM THE TIME DATA STORAGE CAPACITY IS 100 CYCLES
120 PRINT "ENTER SPECIMEN IDENTIFICATION NUMBER AS FOLLOWS"
130 PRINT "EXAMPLE: DX1:BYY239.DAT"
140 INPUT K1$
150 PRINT "ENTER NUMERICAL VALUE OF THE PERCENTAGE OF THE LOAD SCALE"
160 PRINT "EX: ENTER 20 FOR 20% LOAD SCALE"
170 INPUT S1
180 M1=100/S1
190 PRINT "ENTER NUMERICAL VALUE OF THE PERCENTAGE OF THE STRAIN SCALE"
200 PRINT "ENTER 20 FOR 20% STRAIN SCALE"
210 INPUT S2
220 N1=100/S2
230 PRINT "ENTER THE VALUE OF TENSILE CREEP LOAD IN POUNDS"
240 INPUT P0
250 P0=INT(P0*2047*(M1/20000))
260 PRINT "ENTER DIAMETRAL INELASTIC DISPLACEMENT RANGE"
270 INPUT D0
280 D0=INT(D0*4096*(N1/.02))
290 PRINT "ENTER DIAMETRAL DISPLACEMENT RANGE CORRESPONDING TO THE"
300 PRINT "AMOUNT OF CREEP TO BE INTRODUCED"
310 INPUT D5
320 D5=INT(D5*4096*(N1/.02))
330 PRINT "ENTER THE VALUE OF FIRST CYCLE TENSILE LIMIT"
340 INPUT D1
350 D1=INT(D1*2047*(N1/.01))
360 PRINT "ENTER THE VALUE OF TENSILE DIAMETRAL DISPLACEMENT LIMIT"
370 INPUT D3
380 D3=INT(D3*2047*(N1/.01))
390 PRINT "ENTER THE VALUE OF COMPRESSIVE DIAMETRAL DISPLACEMENT LIMIT"
400 INPUT D4
```

CONCP.BAS Listing (Continued)

```
410 D4=INT(D4*20+2*(N1/.01))
420 PRINT "D3",D3,"D4",D4,"D1",D1
430 REM INITIALIZING THE CYCLE COUNTER VARIABLE 'N'
440 N=1
450 REM THE FOLLOWING STATEMENTS SET THE TIME
460 PRINT " ENTER AN INTEGER REPRESENTING THE CURRENT HOUR,"
470 PRINT " BASED ON A 24-HOUR DAY"
480 INPUT U1
490 PRINT " ENTER AN INTEGER REPRESENTING THE CURRENT MINUTE"
500 INPUT V1
510 PRINT " ENTER AN INTEGER REPRESENTING THE CURRENT SECOND"
520 INPUT W1
530 PRINT " ENTER AN INTEGER REPRESENTING THE CURRENT MONTH "
540 INPUT X1
550 PRINT " ENTER AN INTEGER REPRESENTING THE CURRENT DAY OF MONTH"
560 INPUT Y1
570 PRINT " ENTER AN INTEGER REPRESENTING THE CURRENT YEAR "
580 INPUT Z1
590 PRINT "MOUNT TIME DATA STORAGE DISK ON DISK DRIVE "1"(ONE)"
600 PRINT "WHEN FINISHED GO TO 610"\STOP
610 PRINT "IF READY TO START THE TEST TYPE 'YES'"
620 INPUT A$
630 IF A$="YES" THEN 650
640 GO TO 610
650 CALL "STIM"(U1,V1,W1,X1,Y1,Z1)
660 CALL "FG1"(P0)
670 CALL "DACQ"(0,D,0,0)
680 IF D>=D1 THEN 700
690 GO TO 670
700 CALL "FG1"(-2048)
710 CALL "GTIM"(A1,B1,C1)
720 CALL "CNTR"(3)
730 CALL "DACQ"(0,D,0,0)
740 IF D<=D4 THEN 760
750 GO TO 730
```

CONCP.BAS Listing (Continued)

```
760 CALL "FG1"(P0)
770 CALL "GTIM"(A2,B2,C2)
780 PRINT "SAMPLING LOAD P0"
790 CALL "DACQ"(0,P,1,0)
800 IF P>=P0 THEN 830
810 GO TO 790
820 PRINT "SAMPLING D BEFORE WRITING ON THE DISK"
830 CALL "DACQ"(0,D,0,0)
840 D2=D
850 R0=7*N
860 R7=R0-7
870 R6=R0-6
880 R5=R0-5
890 R4=R0-4
900 R3=R0-3
910 R2=R0-2
920 R1=R0-1
930 PRINT "WRITING THE TIME VALUES ON THE DISK "
940 OPEN K1$ FOR OUTPUT AS FILE #F1(700)
950 #F1(R7)=N
960 #F1(R6)=A1
970 #F1(R5)=B1
980 #F1(R4)=C1
990 #F1(R3)=A2
1000 #F1(R2)=B2
1010 #F1(R1)=C2
1020 CLOSE
1030 N=N+1
1040 PRINT "SAMPLING THE STRAIN D AFTER WRITING ON THE DISK"
1050 CALL "DACQ"(0,D,0,0)
1060 D9=D-D2
1070 IF D9>=D5 THEN 1090
1080 GO TO 1050
1090 CALL "FG1"(2047)
1100 CALL "DACQ"(0,D,0,0)
```

CONCP.BAS Listing (Conclusion)

```
1110 IF D>=03 THEN 700
1120 GO TO 1100
1130 END

READY
```

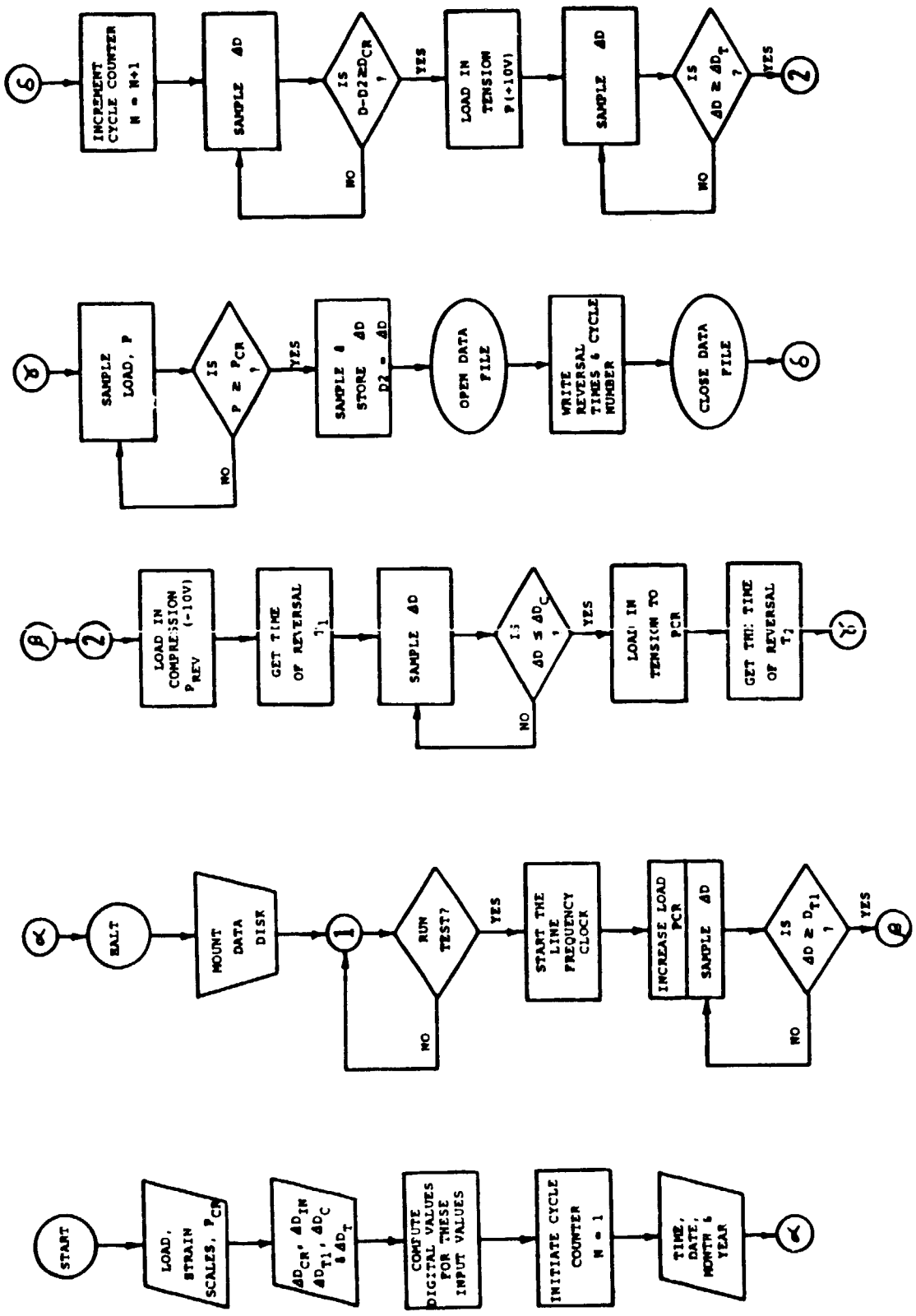

Flowchart for CONCP.BAS Program.

CONSTANT CREEP STRAIN "CP" TEST INPUT DATA FOR CONCP.BAS

1. Specimen Identification Number	: K1$	:
2. Numerical Value of the Percentage of the Load Scale	: S1	:
3. Numerical Value of the Percentage of the Strain Scale	: S2	:
4. Tensile Creep Load in Pounds	: P0	:
5. Diametral Inelastic Displacement Range	: D0	:
6. Diametral Displacement Range Corresponding to the Amount of Creep to be Introduced	: D5	:
7. First Cycle Tensile Diametral Displacement Limit	: D1	:
8. Subsequent Tensile Diametral Displacement Limit	: D3	:
9. Compressive Diametral Displacement Limit	: D4	:
10. Integer representing the Current Hour, based on a 24-hour Day	: U1	:
11. Integer representing the Current Minute	: V1	:
12. Integer representing the Current Second	: W1	:
13. Integer representing the Current Month	: X1	:
14. Integer representing the Current Day of the Month	: Y1	:
15. Integer representing the Current Year	: Z1	:

Sample data input sheet for CONCP.BAS program.

APPENDIX B

Multiple Regression Analysis

Let there be n experimental data points ($n \geq 3$) that are available for the evaluation of the Steady State Creep Rate (SSCR) Modified CP life relationship. Each of these data points contains (a) the generic CP cyclic life N_{cp}, (b) the inelastic strainrange, $\Delta\epsilon_{cp}$ and (c) the steady state creep rate, $\dot{\epsilon}_{ss}$.

The SSCR Modified CP life relationship is of the form

$$N_{cp} = A\left[\Delta\epsilon_{cp}\right]^{\alpha}\left[\dot{\epsilon}_{ss}\right]^{\beta} \tag{B-1}$$

The constants A, α and β are obtained from a multiple regression analysis. Taking logarithms (to base 10) on both sides,

$$\log N_{cp} = \log A + \alpha \log \Delta\epsilon_{cp} + \beta \log \dot{\epsilon}_{ss} \tag{B-2}$$

Error occurring in cyclic life N_{cp} prediction, due to regression analysis,

$$\delta = \log N_{cp} - \log A - \alpha \log \Delta\epsilon_{cp} - \beta \log \dot{\epsilon}_{ss} \tag{B-3}$$

Squaring on both sides,

$$\delta^2 = \left[\log N_{cp} - \log A - \alpha \log \Delta\epsilon_{cp} - \beta \log \dot{\epsilon}_{ss}\right]^2$$

Summing from $i = 1$ to n to add all the squares of the errors occurring at each data point (i.e. $i = 1, \ldots, n$), total of the squares of error

$$\delta^2 = \sum_{i=1}^{n} \delta^2 = \sum_{i=1}^{n} \left[\log\left[N_{cp}\right]_i - \log A - \alpha \log\left[\Delta\epsilon_{cp}\right]_i - \beta \log\left[\dot{\epsilon}_{ss}\right]_i\right]^2 \tag{B-4}$$

To minimize the error in N_{cp}, δ^2 should be minimized with respect to A, α and β.

$$\frac{\partial}{\partial A}\left[\delta^2\right] = 0$$

$$\frac{\partial}{\partial \alpha}\left[\delta^2\right] = 0 \qquad \text{(B-5)}$$

$$\frac{\partial}{\partial \beta}\left[\delta^2\right] = 0$$

Substituting (B-4) into Eqs. (B-5), and then interchanging the summation and differentiation operations, the following equations are obtained.

$$\sum_{i=1}^{n}\left[\left\{\log\left[N_{cp}\right]_i - \log A - \alpha\log\left[\Delta\epsilon_{cp}\right]_i - \beta\log\left[\dot{\epsilon}_{ss}\right]_i\right\} * \left[-\frac{2}{A}\log_{10}^{e}\right]\right] = 0$$

$$\sum_{i=1}^{n}\left[\left\{\log\left[N_{cp}\right]_i - \log A - \alpha\log\left[\Delta\epsilon_{cp}\right]_i - \beta\log\left[\dot{\epsilon}_{ss}\right]\right\} * \left[-2\log\left[\Delta\epsilon_{cp}\right]\right]\right] = 0 \qquad \text{(B-6)}$$

$$\sum_{i=1}^{n}\left[\left\{\log\left[N_{cp}\right]_i - \log A - \alpha\log\left[\Delta\epsilon_{cp}\right]_i - \beta\log\left[\dot{\epsilon}_{ss}\right]_i\right\} * \left[-2\log\left[\dot{\epsilon}_{ss}\right]\right]\right] = 0$$

Since $A \neq 0$, and $\log_{10}^{e}$ and 2 are finite constants they can be cancelled in Eqs. (B-6). After some algebraic manipulation Eqs. (B-6) can be arranged in the following matrix form:

Using the following notation,

$$a_{11} = n$$

$$a_{12} = a_{21} = \sum_{i=1}^{n} \log \left[\Delta\epsilon_{cp}\right]_i$$

$$a_{13} = a_{31} = \sum_{i=1}^{n} \log \left[\dot{\epsilon}_{ss}\right]_i$$

$$a_{22} = \sum_{i=1}^{n} \left\{\log \left[\Delta\epsilon_{cp}\right]_i\right\}^2$$

$$a_{23} = a_{32} = \sum_{i=1}^{n} \left\{\log \left[\dot{\epsilon}_{ss}\right]_i \log \left[\Delta\epsilon_{cp}\right]_i\right\}$$

$$a_{33} = \sum_{i=1}^{n} \left\{\log \left[\dot{\epsilon}_{ss}\right]\right\}^2$$

$$x_1 = \log A$$

$$x_2 = \alpha$$

$$x_3 = \beta$$

$$B_1 = \sum_{i=1}^{n} \log \left[N_{cp}\right]_i$$

$$B_2 = \sum_{i=1}^{n} \left\{ \log \left[N_{cp} \right]_i * \log \left[\Delta \epsilon_{cp} \right]_i \right\}$$

$$B_3 = \sum_{i=1}^{n} \left\{ \log \left[N_{cp} \right]_i * \log \left[\dot{\epsilon}_{ss} \right]_i \right\}$$

$$\begin{bmatrix} a_{11} & a_{12} & a_{13} \\ a_{21} & a_{22} & a_{23} \\ a_{31} & a_{32} & a_{33} \end{bmatrix} \begin{bmatrix} x_1 \\ x_2 \\ x_3 \end{bmatrix} = \begin{bmatrix} B_1 \\ B_2 \\ B_3 \end{bmatrix} \qquad \text{(B-7)}$$

Constants $\log A$, α and β are obtained by solving the system of Eqs. (B-7) simultaneously. For Failure Time (FT) Modified CP life relationship, Steady state creep rate, $\dot{\epsilon}_{ss}$ should be replaced by time to failure t_f in the above analysis.

1. Report No.	2. Government Accession No.	3. Recipient's Catalog No.
NASA CR-174946		

4. Title and Subtitle	5. Report Date
Time Dependency of Strainrange Partitioning Life Relationships	August 1984
	6. Performing Organization Code

7. Author(s)	8. Performing Organization Report No.
Sreeramesh Kalluri and S.S. Manson	None
	10. Work Unit No.

9. Performing Organization Name and Address	11. Contract or Grant No.
Case Western Reserve University Cleveland, Ohio 44106	NAG 3-337
	13. Type of Report and Period Covered
12. Sponsoring Agency Name and Address	Contractor Report
National Aeronautics and Space Administration Washington, D.C. 20546	14. Sponsoring Agency Code
	533-13-01

15. Supplementary Notes

Final report. Project Manager, Gary R. Halford, Structures Division, NASA Lewis Research Center, Cleveland, Ohio 44135.

16. Abstract

The effect of exposure time (or creep rate) on the CP life relationship is established by conducting isothermal CP tests at varying exposure times on 316 SS at 1300 and 1500 °F. A reduction in the CP cycle life is observed with an increase in the exposure time of the CP test at a given inelastic strainrange. This phenomenon is characterized by modifying the Manson-Coffin type of CP relationship. Two new life relationships, (i) the Steady State Creep Rate (SSCR) Modified CP life relationship, and (ii) the Failure Time (FT) Modified CP life relationship, are developed in this report. They account for the effect of creep rate and exposure time within the CP type of waveform. The reduction in CP cyclic life in the long exposure time tests is attributed to oxidation and the precipitation of carbides along the grain boundaries.

17. Key Words (Suggested by Author(s))	18. Distribution Statement
Fatigue (metal); Creep-fatigue; Strainrange partitioning; Life prediction; Ductility; Strain cycling	Unclassified - unlimited STAR Category 39

19. Security Classif. (of this report)	20. Security Classif. (of this page)	21. No. of pages	22. Price*
Unclassified	Unclassified		

*For sale by the National Technical Information Service, Springfield, Virginia 22161